Artigo Original
Original Article

PRÉMIO ROBALO CORDEIRO AER/GSK 2008
ROBALO CORDEIRO AER/GSK 2008 AWARD

Maria Filomena Rabaça Roque Botelho[1]
Maria Alcide Tavares Marques[2]
Célia Maria Freitas Gomes[1]
Augusto Marques Ferreira da Silva[3]
Vasco António Andrade Figueiredo Bairos[4]
Manuel Amaro de Matos Santos Rosa[5]
Antero Pena Abrunhosa[1]
João José Pedroso de Lima[1]

Nanorradiolipossomas modulados molecularmente para estudar a drenagem linfática pulmonar profunda

Nanoradioliposomes molecularly modulated to study the lung deep lymphatic drainage

Recebido para publicação/*received for publication:* 09.01.23
Aceite para publicação/*accepted for publication:* 09.01.26

Resumo

A drenagem linfática pulmonar profunda (DLPP) desempenha um papel importante na remoção de materiais estranhos, constituindo os macrófagos alveolares a primeira linha de defesa fagocitária, dada a grande afinidade para microrganismos patogénicos. Os *Bacillus subtilis* são saprófitas do tracto respiratório humano com ampla utilização em investigação e em biotecnologia.

Abstract

Lung deep lymphatic drainage (LDLD) plays an important role in the removal of foreign materials from lungs being alveolar macrophages the first line of phagocytic defence with high affinity for pathogenic microorganisms. *Bacillus subtilis* is a well-known genome-decoded saprophyte of the human respiratory tract used in research and in the biotechnology industry.

[1] Instituto de Biofísica e Biomatemática, Faculdade de Medicina, Universidade de Coimbra, Azinhaga de Santa Comba, Celas, 3000-548 Coimbra, Portugal
[2] Departmento de Ciências Pneumológicas e Alergológicas, Hospitais da Universidade de Coimbra, Praceta Mota Pinto, 3000-075 Coimbra, Portugal
[3] Departmento de Electrónica e Telecomunicações, Universidade de Aveiro, 3810-193 Aveiro, Portugal
[4] Instituto de Histologia e Embriologia, Faculdade de Medicina, Universidade de Coimbra, Rua Larga, 3004-504 Coimbra, Portugal
[5] Instituto de Imunologia, Faculdade de Medicina, Universidade de Coimbra, Rua Larga, 3004-504 Coimbra, Portugal

Correspondência/*Correspondence to:*
Maria Filomena Botelho
Instituto de Biofísica e Biomatemática
IBILI-Faculdade de Medicina
Azinhaga de Santa Comba, Celas
3000-548 Coimbra
Portugal
Tel: +351 239 480240
FAX: +351 239 480258
Email: filomena@ibili.uc.pt

NANORRADIOLIPOSSOMAS MODULADOS MOLECULARMENTE PARA ESTUDAR A DRENAGEM LINFÁTICA PULMONAR PROFUNDA

Maria Filomena Rabaça Roque Botelho, Maria Alcide Tavares Marques, Célia Maria Freitas Gomes, Augusto Marques Ferreira da Silva, Vasco António Andrade Figueiredo Bairos, Manuel Amaro de Matos Santos Rosa, Antero Pena Abrunhosa, João José Pedroso de Lima

As cadeias linfáticas pulmonares profundas (CLPP) constituem um dos primeiros locais de disseminação de tumores pulmonares.

Neste trabalho pretendeu-se desenvolver e validar um método não invasivo para avaliar as CLPP através de nanorradiolipossomas aerosolisados e modulados pela parede do esporo do *Bacillus subtilis*. O objectivo final foi produzir uma formulação de nanorradiolipossomas capaz de imitar a dinâmica da remoção de esporos pelas CLPP e simultaneamente ter propriedades ideais como traçador para imagiologia molecular.

Testámos sete diferentes formulações lipossómicas, tendo a formulação F demonstrado possuir propriedades fisicoquímicas e radiofarmacêuticas que a tornam o traçador ideal para imagiologia molecular *in vivo* das CLPP.

Os nanorradiolipossomas da formulação F após marcação com ^{99m}Tc-HMPAO foram administrados sob a forma de aerossóis a 20 *Sus scrofa*. Visualizaram-se comunicações hilares e interpulmonares nos primeiros 5 minutos após a inalação, as cadeias infradiafragmáticas entre os 10 e os 20 minutos, os gânglios da cadeia aórtica aos 20 minutos e os da região hilar renal aos 30 minutos.

Em conclusão, o método proposto visualiza os gânglios linfáticos e a rede linfática pulmonar profunda. A modulação dos nanorradiolipossomas permite que eles atinjam órgãos ou tecidos específicos, conferindo-lhes importantes potencialidades no âmbito do diagnóstico e/ou da terapêutica.

Rev Port Pneumol 2009; XV (2): 261-293

Palavras-chave: Nanorradiolipossomas, modulação molecular, drenagem linfática pulmonar, imagem nuclear funcional.

Lung deep lymphatic chains (LDLC) constitute one of the first sites of lung tumours' dissemination.

In this work we intended to develop and validate a non-invasive method for assessing LDLC by nanoradioliposomes aerosolised modulated on the *Bacillus subtilis* spore wall. The final goal was to produce a nanoradioliposome formulation that can mimics the dynamics of preferential removal of spores by LDLD and present the ideal properties as a tracer for molecular imaging studies.

Seven different liposomal formulations were tested, and the formulation-F demonstrated physicochemical and radiopharmaceutical properties that make it an ideal candidate as an *in vivo* probe for molecular imaging studies of the LDLC.

Nanoradioliposomes of the formulation-F after labelling with 99mTc-HMPAO were administered as aerosols to 20 *Sus scrofa*. Hilar and interpulmonary communications were visualized in first 5 minutes post-inhalation, infradiaphragmatic chains between 10 and 20 minutes, the ganglia of the aortic chain at 20 minutes and those of the renal hilar region at 30 minutes.

Conclusion: the proposed method enables visualization of deep lymphatic lung network and lymph nodes. Besides, this technique involving the modulation of nanoradioliposomes targeting specific organs or tissues may be an important tool for diagnostic or even for therapeutic purposes.

Rev Port Pneumol 2009; XV (2): 261-293

Key-words: Nanoradioliposomes, molecular modulation, lung lymphatic drainage, functional nuclear imaging.

Maria Filomena Rabaça Roque Botelho, Maria Alcide Tavares Marques, Célia Maria Freitas Gomes, Augusto Marques Ferreira da Silva, Vasco António Andrade Figueiredo Bairos, Manuel Amaro de Matos Santos Rosa, Antero Pena Abrunhosa, João José Pedroso de Lima

Introduction

Preliminary studies carried out in mongrel dogs (*canis familiaris*), which inhaled *Bacillus subtilis* aerosols labelled with technetium-99m, showed not only a fast disappearance of the pulmonary activity but also the capacity of visualize the lung deep lymphatic network.

The impossibility to use bacilli, even saprophytes, in human beings, gave us the idea of developing radioactive nanoliposomes with membranes molecularly modulated to have a structure similar to the wall of these bacilli. This approach allowed a simulation of their mechanical behaviour in the pulmonary lymphatic network, but without presenting pathogenic effects.

The molecular composition of the *Bacillus subtilis* membrane is already known[1,2,3] and it is possible, to anticipate the structures that are responsible for its dynamic behaviour at the alveolar-capillary membrane.

The development of nanoliposomes with the *Bacillus subtilis* membrane properties and the study of its behaviour in an animal model, after being labelled with ^{99m}Tc-HMPAO, with Nuclear Medicine diagnostic purposes, as well as the interest of the development of a practical and not invasive method of visualization of the lung deep lymphatic chains is of great interest in several pathologic situations of this area, and constitute the main subject of this work.

The molecular modulation of liposomes can lead to the production of cells analogous, or other structures with specific properties, that allows not only the visualization of organs or tissues by the use of radioactive liposomes or liposomes carriers of radiopharmaceuticals, but involves also a therapeutic perspective due to the radiation or pharmacological effects.

The development of liposomal structures with dimensions around 100 nm to which some molecular residues can be aggregate, with biochemists and biological specific properties, could be an important tool in Medicine.

Lung lymphatic system

The lung lymphatic system is of fundamental importance in the alveolar and interstitial clearance, not only immediately after the birth and during the alveolisation, with the fast removal of fluids of the fetal lung, but also during all life long, once a great diversity of substance can reach the pulmonary alveoli, needing to be cleared in order to allow an efficient gas exchange through the alveolar-capillary barrier[4,5,6,7].

The lung lymphatics, as in another organ, consist in collector and capillary lymphatics[4,5,6,7]. The lymphatic collector vessels show valves regularly distributed throughout its length and are the main branches of pulmonary lymphatic drainage, receiving the lymph from the lymphatic capillaries. This lymph is subsequently drained in direction to the lymphatic nodes of the pulmonary hila and to the systemic circulation, after passed through the tracheobronchial, tracheal and paratracheal lymphatic nodes[8].

The lymphatic capillaries are located in the areas of extracellular exchanges with the pulmonary interstitium, allowing a continuous drainage of interstitial fluid, macromolecules and cells[6,7].

The pulmonary lymphatics (Fig. 1) are distributed in two linked networks: the superficial pleural network, located in the sub-mesothelial connective tissue of the visceral pleura and the deep intrapulmonary network, cons-

Maria Filomena Rabaça Roque Botelho, Maria Alcide Tavares Marques, Célia Maria Freitas Gomes, Augusto Marques Ferreira da Silva, Vasco António Andrade Figueiredo Bairos, Manuel Amaro de Matos Santos Rosa, Antero Pena Abrunhosa, João José Pedroso de Lima

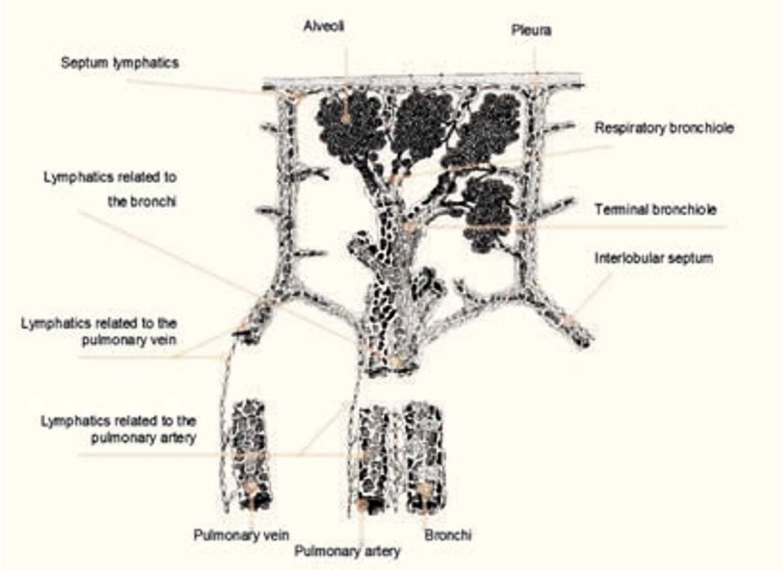

Fig. 1 – Schematic representation of pulmonary lymphatics distribution and organisation. *[Adapted from Nagaishi and Okada]*

tituting the peribronchovascular lymphatics, located in the connective tissue sheets of the pulmonary bronchial and vascular trees[6,7].

The pleural lymphatics, located inside of the pleural sub-mesothelial connective tissue, are organized as a vessel network that runs on the pulmonary surface, in direction to pulmonary hilum where they join to the deep lymphatic network[6,8].

The peribronchovascular lymphatics go around the different airway generations until they reached the respiratory bronchioles, as well as the pulmonary arterial and venous vessels, being the lymphatic drainage parallel to the bronchovascular system.

These two plexus that are interconnected in anatomic terms at hilar and pleural level, in functional terms must remain more or less isolated, because its different valves orientation[4,8].

The superficial lymphatic plexus must transfer the lymph from the pleura and the fine sub-pleural parenchyma adjacent sheet

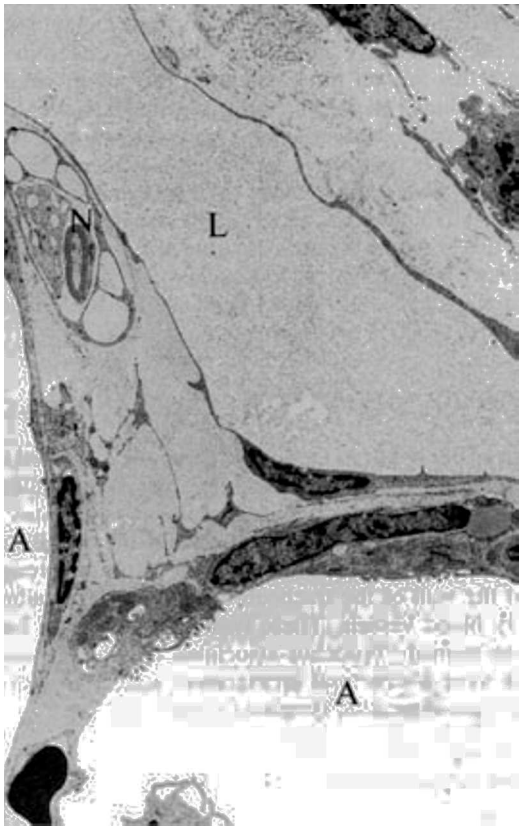

Fig. 2 – Image obtained by electron microscopy, that shows a juxta-alveolar lymphatic capillary (L) contiguous to the alveolar space (A). *[Adapted from Leak and Ferran]*

to the pulmonary hilum, through lung surface, whereas the peribronchovascular plexus drains the remained pulmonary parenchyma throughout the blood vessels and airways ramifications.

Additionally, many lymphatic capillaries are found in the juxta-alveolar regions (Fig. 2), which are contiguous to the alveolar wall, being separate from the alveolar lumen only by alveolar epithelium and support conjunctive tissue, which are very thin and only contains few vessels[4,6,8].

This way, the lung lymphatics are presented in the loose connective tissue that supports

the more peripheral pleural cells that involves the pulmonary lobes, in the interalveolar septa, peribronchial and perivascular sheets.

Theory of the method

The need lung lymphographic studies in man, as it happens in some obstructive lymphatic pathologies, has been fulfilled through a few radiological procedures[9], namely through indirect lymphography.

More recently, the introduction of radioisotopic techniques, allowed performing indirect lymphoscintigraphies with tracers administration through intrapleural, or at peripheral members. These methods are invasive, difficult for the patient and technically hard to perform.

Our approach was to use the dynamic and functional properties of the lung lymphatic system in order to develop a tracer that will be drained by lymphatics after inhalation, and that could be detectable externally with a gamma camera.

Among the several exogenous materials, the inactivated or analogous to pathogenic agents seemed to be a field to explore. Our first choice was the research of an airways saprophyte microorganism, labelling it with a radioactive tracer and administering it as an aerosol and follows its route and posterior localizations.

The selection elicited the *Bacillus subtilis*, which could be used in its vegetative or sporulated forms.

These two forms were labelled with ^{99m}Tc chelated by exametazime (HMPAO) (Ceretec™, G.E. Healthcare, UK) and were administered to dogs as aerosol. Two dogs had received aerosols with vegetative forms, and the other two aerosols with spore forms.

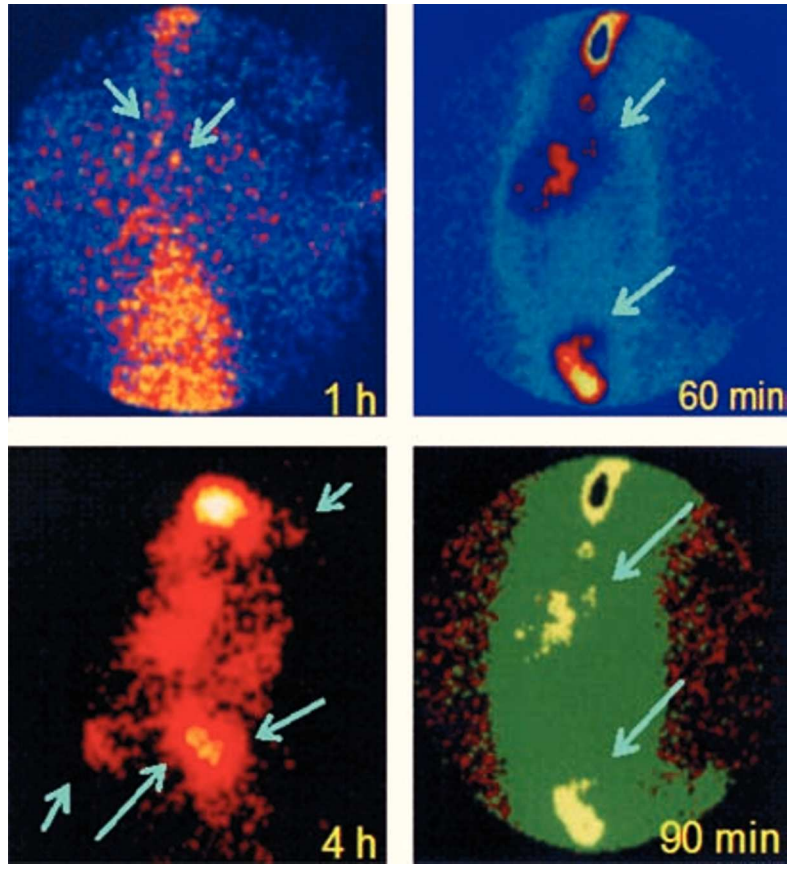

Fig. 3 – Images obtained after *Bacillus subtilis* aerosol administration, as vegetative form (left) and as spores (right) labelled with ^{99m}Tc-HMPAO. In each image is referred the time after inhalation

The images obtained in these 4 animals, revelled the existence of deep lymphatic drainage chains, beginning with appearance of lymphatic nodes located in the neck region, and inguinal level at delayed times. The images obtained were similar with the two different forms, the vegetative and spore forms (Fig. 3).

The utilization in humans of any forms of microorganisms, even saprophyte is clearly out of question. However, we thought that

the production of carriers with walls similar to the molecular structure of cellular membranes of the bacilli, but without any components able to induce host immune responses could be a promising field of research.

So, we tried to obtain a liposomic formulation, which bilayer composition was such that simulate the dynamic behaviour of the *Bacillus subtilis*, without the disadvantages of these, but with the inherent advantages of liposomes, that are: to be inert, to have good tolerance and to be biodegradable.

Keeping in mind the similar *in vivo* behaviour of the two forms of *bacilli*, and the faster lymphatic drainage of the spores form besides its easier manipulation, the spore membrane was used as model of liposomes wall.

The *Bacillus subtilis* spores had a complex composition that can schematically be appreciated in Fig. 4. Basically, the *Bacillus subtilis* spore is constituted by diverse layers of variable composition: the exospore, the dense outer spore coat (DSC), the internal coat (IC), the cortex (Cx), the germ cellular wall (GCW) and the cellular membrane (CM).

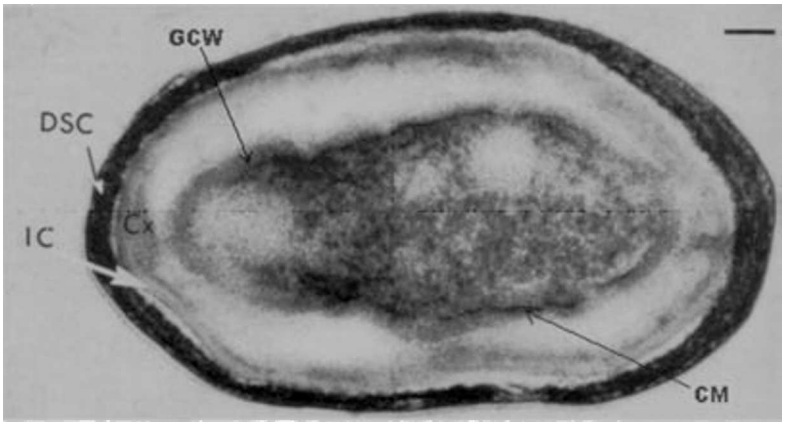

Fig. 4 – Chemical composition of the *Bacillus subtilis* spore. *Exospore*: proteins, phospholipids (cardiolipin)
DSC and IC: proteins (polyglycine II), amino-acids (glutamic acid, lysine, serine); Cx: mucopeptides, peptidoglycans (N-acetyl muramic acid); GCW: mucopeptides; CM: proteins, lipids: neutral lipids, diglycosil diglyceride, phospholipids (cardiolipin, phosphatidylglycerol, phosphatidylethanolamine, e lipo-amino acids) [adapted from www.gsbs.utmb.edu/microbook/ch002.htm]

The exospore, that represents the most outer spore layer, is composed by proteins and phospholipids namely cardiolipin, which is also named as diphosphatidylglycerol.

The dense outer spore coat (DSC) and the internal coat (IC), have in its constitution proteins, where the polyglycine II predominates, and amino acids which the most important are the glutamic acid, the lysine and the serine.

In the spore cortex (Cx) the mucopeptides and the peptidoglycans are predominate, namely the N-acetyl muramic acid.

The germ cellular wall (GCW), sometimes designated as cortical membrane, remains anchored on a few places to the cortex and basically is constituted by mucopeptides whereas the cellular membrane (CM) contains proteins and lipids. Among the lipids, there are great quantities of phospholipids, diglycosil diglyceride and neutral lipids. Related to the spore cellular membrane phospholipids, a clear predominance of cardiolipin exists, besides phosphatidylglycerol, phosphatidylethanolamine and lipo-amino acids such as lysine, alanine, glycine and leucine[1,2,3,11,12].

The study of the Bacillus subtilis spore composition reveals the existence of great amounts of cardiolipin or diphosphatidylglycerol and phosphatidylglycerol that are negatively charged phospholipids.

The value of the negative charge on the liposomes surface is of critical importance, because the pulmonary endothelium acts as a positive barrier. This fact is the opposite to the other endothelia, and several authors,

have proven through studies performed on the lung lymphatic drainage, a faster lymphatic drainage of the anionic compounds than the cationic ones of comparable molecular weight[13].

In order to show a similar behaviour to the *Bacillus subtilis* spores, the wall of the modulated liposome must be constituted by a phospholipid as a main compound associated to a negative charge phospholipid and residues that confers its identical specificity to the Bacillus.

In relation to the main phospholipid, although great part of the liposomes studies as drug carriers uses the dipalmitoyl phosphatidylcholine (DPPC), our option was different because this phospholipid forms particularly unstable liposomes when in contact to biological fluids, releasing about 50% of its aqueous content per hour[14].

As our goal was to get stable liposomes, our option was the distearoylphosphatidylcholine (DSPC), that is a saturated phospholipid with 18 carbons in the two acyl chains that has a phase transition temperature of 56ºC, which makes liposomes much more stable[15-20].

Related to the phospholipid negatively charged, and although cardiolipin (CP) is the predominant lipid of the spore coat of *Bacillus subtilis*[2] its use in humans put some problems due to its immunogenic properties[21]. Therefore, we select the phosphatidylglycerol (PG), that also it has negative charge and is present in the spore coat.

Nevertheless, we made also formulations that contained cardiolipin, for behaviour comparison once it is the predominant phospholipid of the spore coat.

As residues, we used glutamic acid (GA), present in dense outer spore coat and in internal coat and N-acetyl muramic acid (NAMA) an aminosugar present in the peptidoglycan of the spore cortex[11,12].

The introduction of the cholesterol (CL) in the liposomal bilayer was also considered, due to its effect on membrane stabilisation[14,22] preventing the aggregation of the small DSPC vesicles during the storage at 4ºC[17].

We designed and tested 7 different liposomal formulations with the following composition (in parenthesis it is the molar ratio of each component): Formulation A – DSPC:PG:GA [8:1:1]; Formulation B – DSPC:PG:NAMA [8:1.5:0.5]; Formulation C – DSPC: CP: NAMA [8:1:1]; Formulation D – DSPC: PG:CP [8:1:1]; Formulation E – DSPC:PG: CP:CL [7.5:1:1:0.5]; Formulation F – DSPC: PG:NAMA:CL [7.5:1.5:0.5:0.5]; Formulation G – DSPC:CP: NAMA:CL [7.5:1:1: 0.5].

These formulations were evaluated *in vitro* in order to choose the one with better behaviour as radioactive tracer for visualisation of the deep lymphatic lung drainage, after its administration as aerosols.

Materials and methods

Liposomes

Chemicals

The products used for liposome production, i.e., distearoyl phosphatidylcholine (DSPC), phosphatidylglycerol (PG), N-acetyl muramic acid, glutamic acid, cardiolipin, cholesterol and glutathione were obtained from Sigma (St. Louis, MO, USA). ^{99m}Tc was obtained from a commercial ^{99}Mo/^{99m}Tc generator (G.E. Healthcare, UK). Exametazime or HMPAO (Ceretec™)

was purchased from G.E. Healthcare (UK). Sephadex G-25 was obtained from Pharmacia (Upsala, Sweden). Azoperone (Yanssen Pharmaceutical, Belgium) and Ketalar™ (Parke Davis Co, Spain) were used for induction and full anaesthesic purposes, respectively. Diazepam (MediBial, Portugal) was used for myorelaxation during surgical procedures. Strips of ITLC-SG (Instant thin-layer chromatography – silica gel) was obtained from Gelman Sciences Inc., Ann Arbor, USA and Whatman no. 1 paper (Whatman, UK) were used for chromatographic evaluation of labelling efficiency and radiochemical purity. All chemicals and reagents not specified in the text were of analytical grade or equivalent.

Preparation of liposomes

Liposomes were prepared according to the seven formulations listed above, without further purification of the lipids.

Typically, mixtures of the appropriated lipids, in concentration of 50mg/ml, were dissolved in 2 ml of chloroform in a round-bottom flask, and the lipid solutions were rotary evaporated to dryness at room temperature, under reduced pressure and inert atmosphere, for about 2 hours, to form a thin lipid film, which had been dried in vacuum overnight[17,21]. Following complete chloroform evaporation, the lipid mixture films were hydrated with 100 mM reduced glutathione (GSH) in 0.9% saline by vigorous vortex mixing[22-25]. Next, the round-bottom flask was placed in a 65ºC water bath for 10 min. This procedure (heating followed by vigorous mixing) was repeated twice, allowing the formation of multilamellar liposomes.

The multilamellar liposomes were then extruded at 70ºC through two stacked polycarbonate filters (Nucleopore, CA, USA) of 100 nm pore size, mounted in a mini-extruder (LiposoFast™, Avestin, Canada) fitted with two 0.5 ml Hamilton syringe (Hamilton, NV, USA)[26-28]. The samples were subjected to 20 passages through the filters, to form unilamellar liposomes, with a small polydispersity index.

After processing, the vesicle suspension was eluted through a Sephadex G-25 gel molecular exclusion chromatography minicolumns at room temperature, to remove any extravesicular GSH[29-32].

The minicolumns were mounted in 1 ml tuberculin syringe tubes, plugging the barrel with a small durapore® membrane filter (Millipore, Ireland) with a 0.45 µm pore size, and filling the syringes with Sephadex G-25 gel until the 1 ml mark. For the separation, the columns were pre-washed with 0.9% saline, pH=7.4, with a flow rate of approximately 21 ml/h and samples of 500 µl of vesicle solution from each formulation were applied to the minicolumns[17,28,33].

Labelling of liposomes

For the labelling procedure, a modified methodology based on that described by Phillips et al. was used[22,25,34,35].

HMPAO kits, containing 0.5 mg exametazime, 7.6 µg $SnCl_2$ and 4.5 mg NaCl were reconstituted with 740 MBq (20 mCi) of ^{99m}Tc pertechnetate freshly eluted in 1 ml of 0.9% NaCl solution and incubated for 5 min at room temperature.

The reconstituted kits were checked for the presence of primary lipophilic ^{99m}Tc-HMPAO complex and for contamination by

free pertechnetate, reduced hydrolysed ^{99m}Tc and secondary hydrophilic ^{99m}Tc-HMPAO complex using a three step thin-layer ascendant chromatography system, as recommended by the manufacturer. According to the manufacturer's recommendations for cerebral blood flow studies, only kits where the primary lipophilic HMPAO complex was greater than 80% were used for liposome labelling. ^{99m}Tc-HMPAO was then added to 1.5 ml of each GSH containing liposome formulation and incubated at room temperature, for 30 min.

After the incubation period, liposomes were separated from any contaminant by passage through a second Sephadex G-25 gel mini-column, prepared as referred above.

The labelling efficiency of ^{99m}Tc-HMPAO-liposomes was checked by instant thin layer chromatography – silica gel (ITLC-SG) developed in 0.9% saline. With this system, the liposomes remain at origin, while the contaminants move with the solvent front[36-38].

In order to verify that the ^{99m}Tc-HMPAO was in the liposome aqueous phase, during the second Sephadex G-25 gel molecular exclusion chromatography, 120 eluted fractions of 250 µl were collected and analysed for radioactivity.

Liposomes size and surface charge measurements

The vesicle size distribution was determined by quasi elastic light scattering analysis, using a Coulter N4 Plus. Quasi elastic light scattering, also referred to dynamic light scattering or photon correlation spectroscopy, employs digital self-correlation to analyse the fluctuations in scattered light intensity generated by the diffusion of vesicles in solution[39-41]. The measured diffusion coefficient was used to obtain the average hydrodynamic radius and, hence, the mean diameter of the vesicles[14,42].

The surface charge of the liposomes was determined by laser Doppler velocimetry using a Coulter Delsa 440, which performed measurements at 4 light incidence degrees: 34.7º, 26º, 17.4º and 8.7º. These data allowed the calculation of the electrophoretic mobility and zeta potential of the samples.

Stability studies

The temporal wall integrity of the different liposomal formulations was evaluated *in vitro* by ascendant microchromatography. In this system, a decrease on labelling efficiency represents a loss of aqueous liposomal content, which is an indicator of wall integrity.

Strips of ITLC-SG with saline as mobile phase were used, to evaluate the disruptive effects of biological fluids on the wall of the different liposomal formulations.

Liposome stability was determined by incubating at 37ºC a sample of each different radiolabelled liposomal formulation in saline, human serum, human plasma and human serum albumin solution (4mg/ml). Solutions were tested fresh and after incubation at 56ºC for 30 min with the purpose of deactivating the complement of blood fractions. The saline and human serum albumin solutions were used for cross control[14,43].

As an additional confirmation of stability, the aqueous liposomal content loss was checked, every 30 minutes, until 5.5 hours after the second Sephadex G-25 gel molecular exclusion chromatography. Analysis was

done using the ITLC-SG/saline system described above.
As the liposomes will be administered as aerosols, the effect of the 2.7 MHz ultrasound on the integrity of the liposomal wall was also checked. Samples of the different formulations were analysed by microchromatography, using the system previously described, before and after 3 min nebulisation[44,45,46].

Aerosol production
An ultrasonic nebuliser (Heyer Ultraschall Verebler 69, Germany) generating ultrasound (US) of 2.7 MHz frequency was used for aerosol production. The water used in the reservoir was cooled down to 5-6ºC in order to minimise the effects of temperature increase during aerosolisation.

Toxicity
Liposomal cytotoxicity was studied in a human lymphomonocytic population. Cells were incubated with and without the liposomal formulations at different concentrations during 4 hours at 20ºC. After, the cells were labelled with membrane markers (CD3, CD14 and HLA-DR) and incubated during 10 min at 20ºC. Cells were then washed with PBS and analysed by flow cytometry.
In terms of radiotoxicity, the absorbed doses were calculated by the absorbed fraction method, applying the MIRD (Medical Internal Radiation Dose Committee) rules[47,48].

Molecular modulation studies
In order to establish the comparison between the *Bacillus subtilis* spore and liposomes walls, a specific program of molecular modulation (CACHE, Molecular Oxford) was applied. With this program the stearic structures corresponding to the minimum of potential energy were calculated, as for the wall of *Bacillus subtilis* spores and for the wall of liposomes.
For the calculation of the Van der Walls radius, we used an algorithm of molecular mechanics minimisation, named MM2.

In vivo studies

Material
In the scanning electron microscopy (SEM) studies we used a scanning electron microscope Jeol T330 for the evaluation in an adult male Wistar rat.
To accomplish the *in vivo* dynamic studies, we used 20 pigs (*Sus scrofa*). For the image acquisition, a gamma camera General Electric 400 AC (G.E. Healthcare, Milwaukee, USA), controlled by a Genie ACQ computer, running on compatible platform IBM was used.
The data were processed in a dedicated workstation Hewlett Packard (Genie P & R), which runs in an UNIX platform. The samples were weighted in a precision scale (Precisa 205A Superbal-series) and counted in a well count (DPC-gamma C-12, Los Angeles, USA)

SEM studies
For the visualization of the deep lymphatic drainage, the modulated liposomes must reach both the juxta-alveolar lymphatic vessels and the lymphatic capillaries associated to the respiratory bronchioles, i.e. the lipo-

somes must reach the respiratory area of the lung. We choose the inhalatory administration as an aerosol, produced by an ultrasonic nebuliser, with a frequency of 2.7 MHz, once targeting the lung exchange area is much more dependent on the size of aerosol droplets than the liposomes diameter, since they are smaller[44,45].

For the confirmation of the liposomes deposition on the alveolar epithelium administered by inhalation, SEM studies were carried out on an adult male Wistar rat after aerosol inhalation of F formularization liposomes.

Twenty minutes after inhalation, and under deep anaesthesia, the rat thorax was opened and the vascular compartment perfused with saline at 37ºC, with a flow rate of 7 ml/min, by injection in the right ventricle. After, an aortotomy at abdominal level was performed, in order to purge the perfusion liquid. The vascular flush out take about two minutes, until the perfusion liquid became clear. After, a fixation solution of formaldehyde 4%, v/v, in phosphate buffer 0.1 *M*, pH = 7.4 at room temperature, was perfused during 3 – 5 minutes, maintaining the animal condition and perfusion access.

After fixation, lung samples with dimensions of about 3x3x3 mm were taken, which were immerse in a solution of formaldehyde 4%, v/v, in phosphate buffer 0.1 *M*, pH = 7.4. The samples dehydration was performed with acetone, as substitution mean, in successive passages with increasing concentrations since the 20% v/v to 100% v/v. Afterwards, the samples had been dried by CO_2 critical point, in an unit 3000 CP (Polaron), equipped with a high-pressure and temperature manometer, being the temperature variation inside of the chamber assured by circulated boiled water (Thermed 5001 – GLF). Finally, the samples were placed in copper supports by glue with silver (Electron Microscopy Sciences), to be gold coated by cathode evaporation (Polaron). The samples observation was carried out in the scanning electron microscope Jeol T330, selected to the capture of secondary electrons and submitted to a 15 kV of potential difference.

Lymphoscintigraphic studies

For the *in vivo* lymphoscintigraphic studies, liposomes labelled with ^{99m}Tc-HMPAO were administered through inhalation to a 20 *Sus scrofa*.

For these studies, the *Sus scrofa* had been submitted to an anaesthetic protocol consisting of an anaesthetic induction with 40 mg of azoperone by intramuscular injection, immediately followed by intravenous infusion of ketamine hydrochloride (35 mg/kg). For muscle relaxation we used diazepam (10 mg by intramuscular injection). During all procedures, the animals had an intratracheal tube of 4 mm of diameter inserted in the trachea and were kept in spontaneous breath with a mixture of air enriched with therapeutic oxygen. During all the study, the animals kept a nasogastric tube, in order to guarantee the non deglutition of secretions, and consequently the non contamination by digestive route. The bladder of all animals was catheterised in order to maintain the bladder free of urine during all the study.

After aerosols administration, a dynamic acquisition, at thoracic level in posterior view was carried, through the gamma camera coupled with a high resolution parallel hole

collimator, of 120 images of 64×64 pixels, with an individual duration of 30 seconds. After this sequence, static images of 128×128 pixels at thoracic and abdominal levels were acquired at 60, 90, 120, 150, 180, 210 and 240 minutes after the inhalation.

The images acquired with liposomes labelled with ^{99m}Tc-HMPAO, were processed with homemade software specially developed for this study. With this processing, each image is submitted to a subtraction of the lung activity corresponding to the respective time, considering the effective half-life of liposomes. This subtraction allows evidencing the lymphatic nodes.

For comparison of the images acquired after inhalation of labelled liposomes, one pig inhaled an aerosol of native HMPAO labelled with technetium-99m. After this inhalation, a dynamic acquisition was performed, at thoracic level, during 20 minutes, for matrix of 64×64 pixels, 6 images per minute, followed of static images of the thorax and abdomen, of 128×128 pixels at 20, 30, 45 and 60 minutes after the inhalation too.

To confirm the localization of the lymphatic abdominal nodes, two pigs were injected in the first interdigital space of both posterior members, with nanocolloids of human albumin (Nanocoll, Amersham-Sorin, Italy) labelled with ^{99m}Tc, which is a specific tracer for the lymphatic drainage and lymphatic nodes. Immediately after the injection, a dynamic acquisition at abdominal level, in anterior view, of 120 images of 64×64 pixels with individual duration of 30 seconds, was performed. After this sequence, static images of 128×128 pixels at 60 and 90 minutes after interdigital injection were acquired.

Also to confirm the lymphatic abdominal nodes, two animals had been submitted to an interdigital injection, in the left posterior member, of methylene blue dye that is drained by lymphatic system. These animals had been submitted to a laparotomy with abdominal dissection, for direct visualization of the lymphatic vessels (Fig. 5).

For cross control of *in vivo* liposomes stability, in eight pigs during the image acquisition, urine samples and blood samples at 5 min, 30 min, 1, 2, 3, 4, 5 and 6 hours had been collected.

These samples were weighed, counted in a well counter and the specific counts were calculated and converted into % of the administered activity, considering 100% the maximum of the pulmonary activity. The goal was to infer the leak of the water content of the liposomes, once this content is

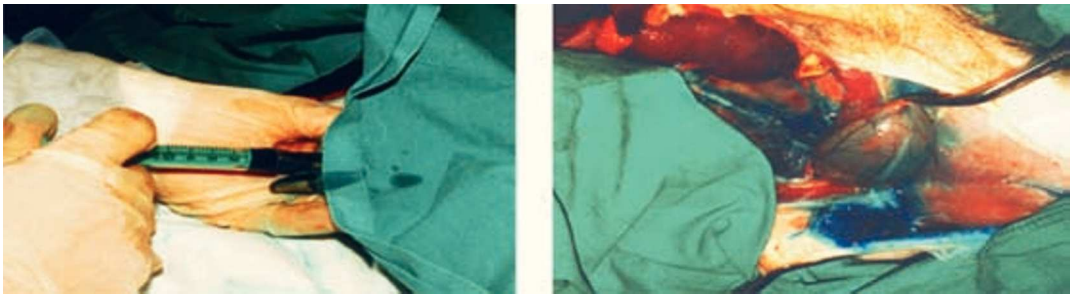

Fig. 5 – Interdigital injection of methylene blue in interdigital space of the left posterior member (left) and explorative laparotomy with visualization of lymphatic drainage (right)

hydrosoluble and would pass to the blood and then, excreted by renal system.
We also wanted to verify, through the images, if there was any localizations corresponding to the presence of liposome in the systemic circulation through venous return, as well as the activity concerning the loss of the liposomes water content, as a consequence of wall liposomal degradation. For this purpose, in the acquired images, we drew regions of interest (ROIs) in some areas (lung, liver, interpulmonary area, abdominal aorta, renal area and bladder projection area) on the times corresponding to the blood collection. For each ROI, the % of activity was calculated, considering the 100% the maximum of the pulmonary activity.

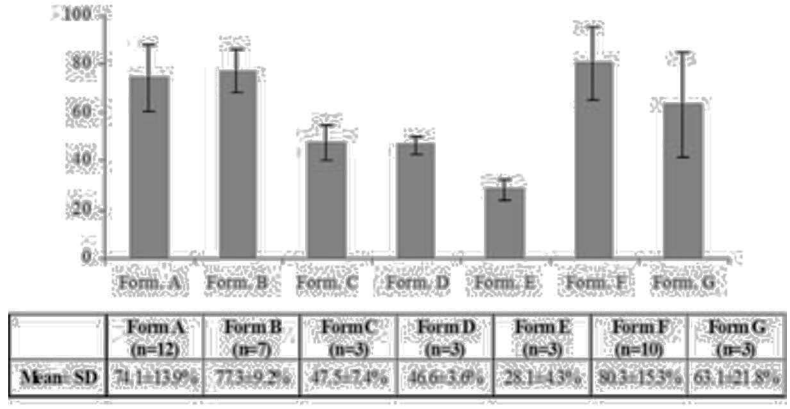

	Form A (n=12)	Form B (n=7)	Form C (n=3)	Form D (n=3)	Form E (n=3)	Form F (n=10)	Form G (n=3)
Mean SD	74.1±13.9%	77.3±9.2%	47.5±7.4%	46.6±3.6%	28.1±4.3%	80.3±15.3%	63.1±21.8%

Fig. 6 – Labelling efficiency (mean ± SD) of the seven liposomal formulations. The labelling efficiency of the 99mTc-liposomes was evaluated by instant thin layer microchromatography – silica-gel (ITLC-SG) with saline as solvent. In this system, the liposomes remain in the origin, while the contaminants go with the solvent front.

Statistical methods

Data were reported as mean ± standard deviation. For comparison of the group results, t-Student analysis was applied to the means. The accepted probability for a significant statistical difference was $p<0.05$.

Results

Liposomes

Our rationale was to develop liposomes with similar physical properties to the genus Bacillus, once is recognized its preferential lymphatic drainage when present in human respiratory system.
We started with seven formulations, with the purpose to obtain at least one formulation characterized by good stability, easiness to label and with good specificity for the lung lymphatic. We used the membrane of the Bacillus subtilis spore as a model, once our previous experience in dogs showed its potential as a tracer of lung lymphatics.
The labelling efficiencies for the seven different developed formulations are presented in Fig. 6.
Ascendant chromatography in ITLC-SG/saline clearly demonstrates the different ^{99m}Tc-HMPAO labelling efficiencies for the various liposomal formulations. Formulation A = 74.1±13.9%; formulation B = 77.3±9.2%; formulation C = 47.5±7.4%; formulation D = 46.6±3.6%; formulation E = 28.1±4.3%; formulation F = 80.3±15.3%; formulation G = 63.1±21.8%.
These differences are related with the lipid composition of the liposomal bilayer. The liposomal formulations with cardiolipin showed the worst results. Oppositely, the presence of an amino sugar associated with cholesterol, even in small percentage, increases significantly the radiolabelling efficiency.
In vitro stability studies were done in saline, human serum, human plasma and human

Table I – Labelling efficiencies (%) for the different liposomal formulations in presence of different fluids (saline, human serum, human plasma, human albumin solution), before and after heating at 56ºC during 30 min, for blood fractions complement inactivation

	Form A (n=7)	Form B (n=7)	Form C (n=3)	Form D (n=3)	Form E (n=3)	Form F (n=7)	Form G (n=3)
Saline	56.9±5.9	69.9±6.8	47.5±7.4	46.6±3.6	28.1±4.3	60.7±10.3	63.1±21.8
Saline 56ºC	49.8±2.9	70.0±2.9	48.7±8.0	34.9±12.6	22.3±3.5	64.6±9.3	47.1±3.4
Human serum	61.1±3.2	76.6±5.5	37.4±10.0	37.7±13.3	21.6±5.7	65.9±4.1	51.3±14.8
Human serum 56ºC	57.0±5.7	77.4±9.5	25.2±5.6	40.4±14.7	22.1±4.9	68.4±9.2	55.6±12.7
Human plasma	58.9±4.5	76.0±3.2	23.8±8.1	40.1±12.4	18.5±5.0	62.3±3.0	51.6±10.2
Human plasma 56ºC	52.9±5.7	72.5±5.8	26.4±4.0	46.4±12.4	19.2±3.1	65.5±6.2	44.3±11.4
Albumin	50.9±6.5	66.3±6.5	31.0±13.3	42.3±21.3	–	59.0±4.9	66.8±4.5
Albumin 56ºC	51.4±8.8	67.6±8.5	18.9±3.2	51.5±11.4	17.6±4.6	63.3±7.7	47.1±16.4

serum albumin solution (4mg/ml) incubated at 37ºC, before and after 30 min heating at 56ºC to inactivate the complement of blood fractions. The results showed that formulations C, D and E besides its small labelling efficiency, presented a lower degree of stability in the presence of biological fluids (Table I).

The results obtained for the labelling efficiency with ^{99m}Tc-HMPAO and the *in vitro* stability in the presence of human serum, human plasma and albumin solution showed that formulations C, D and E presented not only some difficulties in labelling with this method but also showed some instability in the presence of the biological fluids.

As a result, these formulations were excluded from further testing, once the stability in presence of biological fluids was required if the liposomes will be used, in the future, as lung lymphatic tracers. Formulation G, was also excluded because its content in cardiolipin, considered an immunogenic lipid. At this stage, only the three remaining formulations (A, B and F) presented potentialities of usage for our objective.

On the other hand, as the final goal was to administrate the liposomes as aerosols, produced by ultrasonic nebulisation, the three formulations A, B and F were submitted to ultrasounds 2.7 MHz frequency for three minutes, to evaluate their action during aerosol production. The effect of ultrasound action in the stability of the labelled vesicles is shown in Table II.

These results indicate that for ultrasonic nebulisation at 2.7 MHz, there are no statistically significant differences in the stability of the three liposomal formulations, although formulation B appears to be the most affected and Formulation F presents the best results.

Fig. 9 shows the time course of aqueous liposomal content loss during 5.5 hours after the second gel chromatography.

Table II – Labelling fraction of the liposomal formulations A, B and F, before and after 2.7 MHz ultrasounds(US) action during three minutes

	Form. A (n=9)	Form. B (n=4)	Form. F (n=7)
Before US	80.1 ± 10.1%	82.8 ± 6.6%	88.7 ± 6.5%
After US	79.9 ± 10.3%	68.3 ± 24.6%	85.7 ± 5.4%

Maria Filomena Rabaça Roque Botelho, Maria Alcide Tavares Marques, Célia Maria Freitas Gomes, Augusto Marques Ferreira da Silva, Vasco António Andrade Figueiredo Bairos, Manuel Amaro de Matos Santos Rosa, Antero Pena Abrunhosa, João José Pedroso de Lima

The evaluation of the three formulations, using an ITLC-SG/saline microchromatographic system for quantification of loss of radioactive fragments, which migrate with the solvent front, shows that although all formulations lose some of their content over time, formulation F appears to be the most stable.

Based on these results, formulation F was selected as the most promising candidate and was subjected to further tests to assess its suitability as an in vivo imaging agent.

The lipid bilayer of this formularization, based on the composition of the different coats of the *Bacillus subtilis* spores, is constituted by DSPC, PG, NAMA and CL with the following molar ratio 7.5:1.5: 0.5: 0.5.

To test non-encapsulated ^{99m}Tc-HMPAO, radiolabelled liposomes from the F formulation, were submitted then to a second Sephadex G-25 gel molecular exclusion chromatography and 120 eluted fractions of 250 µl were collected and analysed for radioactivity. As it can be observed in Fig. 10, the first 10 fractions, that included the liposomal fractions, accounted for around 85 % of the total activity. The remaining activity (about 15%), considered as being the non-encapsulated tracer, was eluted with the remaining fractions (Fig. 8).

To determine the vesicle size distribution, lipid concentrations of 50 mg/ml were passed 20 times through two stacked polycarbonate membranes of 100 nm pore size. Photon correlation spectroscopy studies indicated a mean diameter of 124.0 ± 32.1 nm and a polydispersity index of 0.09 (n = 3) (Fig. 9).

Electrophoretic mobility and zeta potential determinations of similar samples, obtained by laser Doppler, led to values of 4.1 ± 0.2

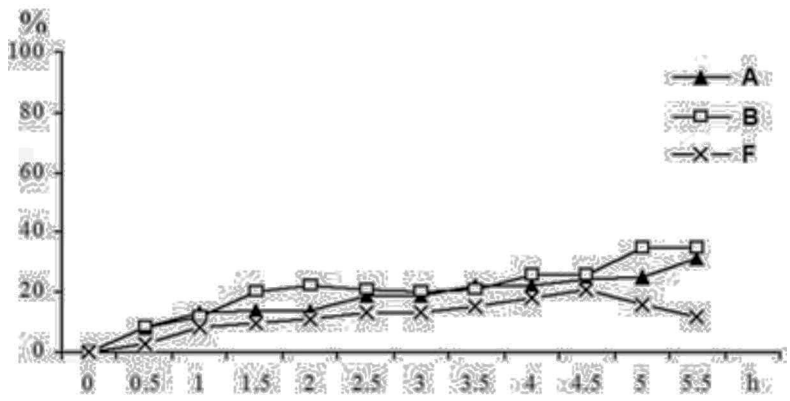

Fig. 7 – Temporal evaluation of the losses of liposomal aqueous content for the formulation A (n=12), B (n=7) and F (n=10) by ascending microchromatography (ITLC-SG/saline)

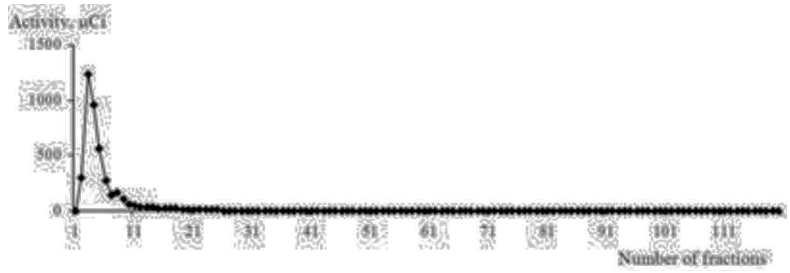

Fig. 8 – Chromatography in column of Sephadex G-25 of liposomes of F formularization (n=4). Samples of 500 µl of the liposomal suspensions had been placed in each column and eluent fractions of 250 µl were collected. This graph represents the activity of each fraction *vs.* number of fractions

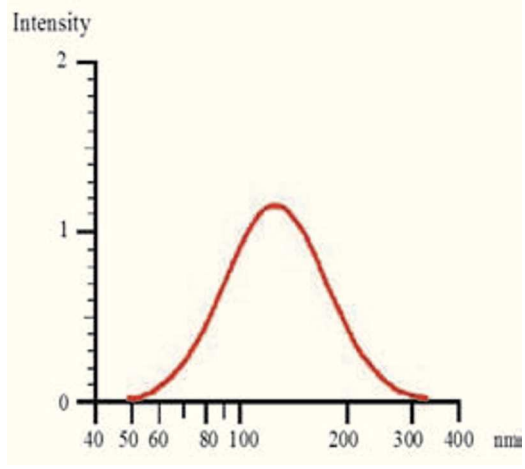

Fig. 9 – Unimodal analysis of the liposomes diameter distribution

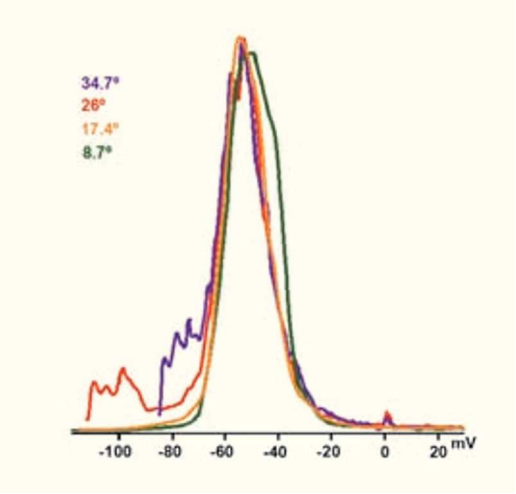

Fig. 10 – Distribution of the zeta potential for the different angles of incidence of the laser

μm cm V^{-1} s^{-1} and 52.8 ± 3 mV respectively (n = 3) (Fig. 10).

In order to evaluate possible ageing effects on this formulation, the samples were left for 6 months at 4ºC before being retested. The results for the different parameters, i.e., mean diameter (150.6 ± 48.2 nm), polydispersity index (0.17), electrophoretic mobility (4.2 ± 0.6 μm cm V-1 s^{-1}) and zeta potential (53.5 ± 6.6 mV) do not show statistically significant differences when compared with the values obtained with fresh liposomes.

The evaluation of cytotoxic effects in a human lymphomonocytic population, by flow cytometry, demonstrated that formulation F in high concentrations appears to modify the ratio of mononuclear cells, inducing a decrease in the total number of lymphocytes. However, in spite of the decrease in the autofluorescence the lymphocytes are not activated as it is showed by the CD3 expression. The monocytes seemed to have some activation, as shown by the analysis of CD14 expression. On the other hand, in small concentrations, the F formulation liposomes did not induce any alteration in the distribution or activation of the two mononuclear lines. In conclusion, the cytotoxicity test was considered negative and the aggressiveness of the formulation F liposomes estimated as being very low (Fig. 11).

In terms of radiotoxicity, for an activity of 111 MBq deposited over the alveolar-capillary membrane, during the inhalation of the ^{99m}Tc-Liposomes, the absorbed dose was calculated by the fractional method using standard MIRD rules[38-39]. The absorbed dose was shown to be in the same order of

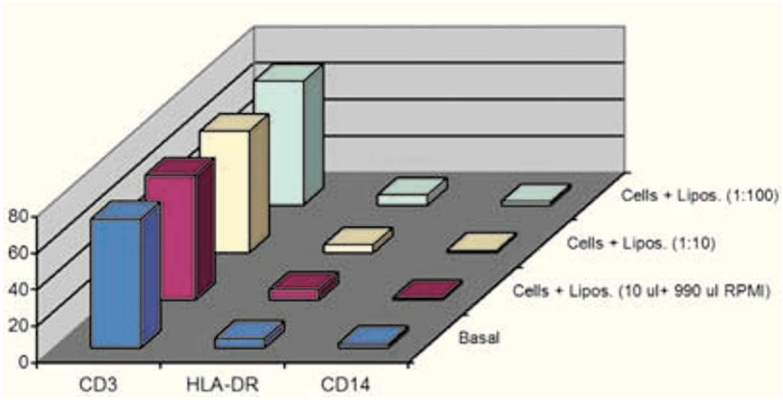

Fig. 11 – Distribution of the cellular markers for the some cultures carried out with the some membrane markers

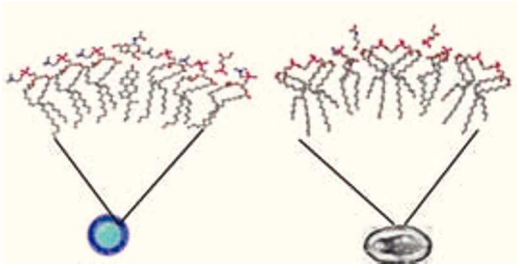

Fig. 12 – Stearic structures of the liposomes wall of formularization F (on the left) and *Bacillus subtilis* spore wall (on the right), corresponding to the minimum potential energy, obtained by a specific software of molecular modulation

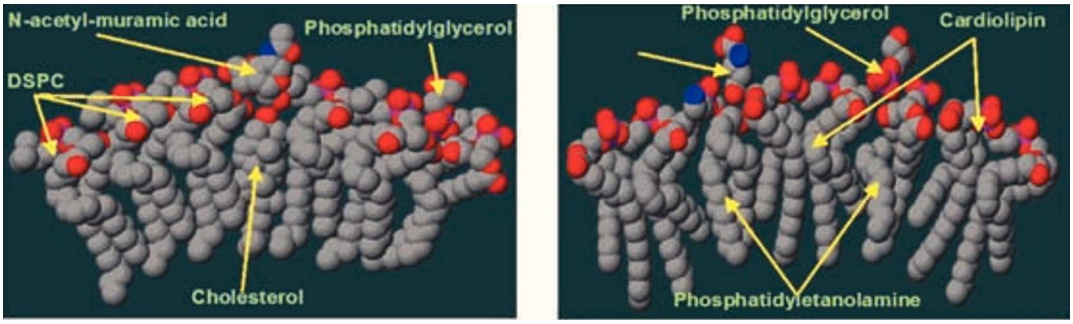

Fig. 13 – Van der Walls radium of liposomes wall of formularization F (on the left) and the *Bacillus subtilis* spore wall (on the right), obtained through an algorithm of energy minimization. We can observe the similar molecular compaction.

magnitude as the obtained with routine Nuclear Medicine studies for the evaluation of alveolar-capillary permeability.

After *in vitro* evaluation of liposomes of formulation F, which showed to be suitable for our purpose, we wanted to analyze based on the knowledge of its complete composition, the ternary and quaternary structure of the liposomes wall in order to compare them with the *Bacillus subtilis* spore wall. To achieve this goal the stearic structures corresponding to the minimum potential energy were calculated for both, Fig 12.

Applying an algorithm for molecular mechanics minimization, the calculation of the Van der Walls radium showed that the molecular compaction of these two structures seemed to be similar, Fig. 13. Additionally, the hydrophilic surface terminations were also alike.

In vivo studies

Scanning electron microscopy

In order to confirm that the liposomes were deposited on the alveolar epithelium, we submitted a Wistar rat to an aerosol inhalation of a solution containing liposomes of formularization F. As we can observe on Fig. 16, twenty minutes after the liposomes inhalation, they are deposited on the lung alveolar surface. We can also verify that they are homogeneously distributed all over the alveolar surface.

Once they reach the alveolar epithelium, the liposomes seem to be phagocyted by the alveolar macrophages and after, drained by the lymphatic channels (Fig. 15).

In spite of this evidence, we cannot exclude the possibility of the direct passage of liposomes through the intercellular spaces, as appears to be the situation showed in the Fig. 14.

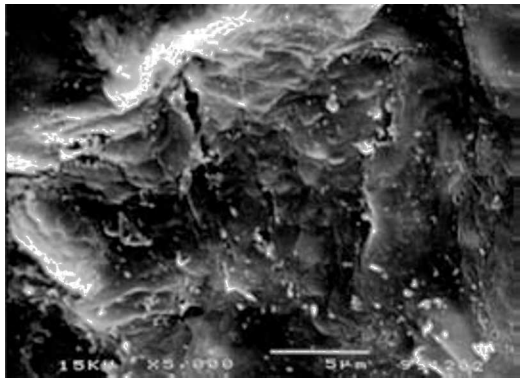

Fig. 14 – SEM image, obtained twenty minutes after the liposomes of formularization F aerosol inhalation. We can see its homogeneous distribution on the alveolar surface

Maria Filomena Rabaça Roque Botelho, Maria Alcide Tavares Marques, Célia Maria Freitas Gomes, Augusto Marques Ferreira da Silva,
Vasco António Andrade Figueiredo Bairos, Manuel Amaro de Matos Santos Rosa, Antero Pena Abrunhosa, João José Pedroso de Lima

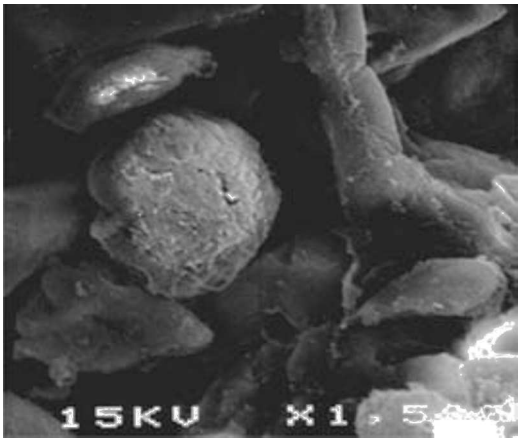

Fig. 15 – SEM image showing a liposome being phagocyted by an alveolar macrophage

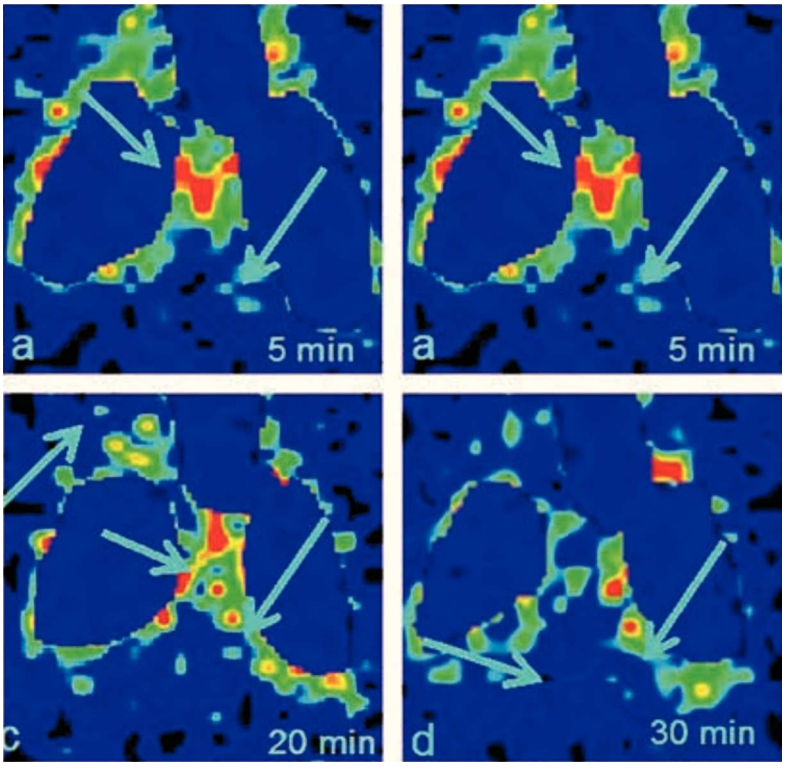

Fig. 16 – Thoracic images in posterior view after 99mTc-Liposome aerosol inhalation, in the pig nº 23. a) 5 min after the inhalation – Visualization of hilar drainage; b) 9 min after – transdiaphragmatic drainage; c) 20 min – initial visualization of aortic chain; d) 30 min – renal hilar ganglia

Lymphoscintigraphy studies

When we analyse the images obtained during the dynamic acquisition in the 20 pigs, without any image processing, we can already observe interpulmonary communications in the images obtained in first 5 minutes, and infradiaphragmatic nodes between the 10 and the 20 minutes. We can also visualise some other abdominal localisations after the first 20 minutes. After image processing, these evidences were more significant.

In the Fig. 16 corresponding to the pig number 23 we can see, in the image obtained at thoracic level, 5 minutes after the inhalation of modulated liposomes, the hilar and interpulmonary lymphatic channels as well as the initial transdiaphragmatic drainage (Fig. 16-a). Nine minutes after the inhalation, the interpulmonary drainage is more individualised and the transdiaphragmatic one is already patent (Fig. 16-b). At 20 min the periaortic ganglia starts to be apparent (Fig. 16-c). At 30 minutes ganglia of renal hilum were visualized (Fig. 16-d) and after 60 minutes the bladder area was already evident.

The study carried out with HMPAO labelled with ^{99m}Tc aerosols, in another animal, in order to compare the images acquired after inhalation of labelled liposomes does not show any type of lymphatic ganglia, in spite of the dispersed abdominal activity, with individualization of the liver and the kidneys (Fig. 17).

The images obtained during the indirect lymphoscintigraphy carried out with nanocolloids of human albumin labelled ^{99m}Tc, in order to confirm the localization of the abdominal lymphatic ganglia show that, 17 minutes after the interdigital injection and

passive movements, the lymphatic trunks of the inferior members were visualised. In the studies performed, the popliteal ganglia were systematically visualized before 30 minutes, usually at 25 minutes and the ganglia of the aortic chain after 30 minutes (Fig. 18).

In Fig. 19, we can see the images of the thoracic region in posterior view and the abdominal region in anterior view both obtained 1 hour and 1.5 hours after labelled liposomes inhalation, concerning the animal n^{er} 23. As we can observe, the infradiaphragmatic, right renal hilum, pelvic region and bladder area localizations are apparent.

In the delayed scintigraphic images, obtained at 2 and 3 hours after inhalation, we visualize more intensively the same projection areas (Fig. 20).

To confirm the abdominal lymphatic ganglia by direct visualization, two animals were submitted to an indirect lymphography obtained after interdigital injection in the left posterior member of methylene blue, a dye that is drained by lymphatic vessels, followed by abdominal laparotomy. In Fig. 21, we can see the early images of the direct abdominal and pelvic region visualization of the animal n^{er} 23, after interdigital injection of the referred dye. We can notice 2 areas coloured in blue, one behind the bladder and another one in the abdominal wall just over the bladder.

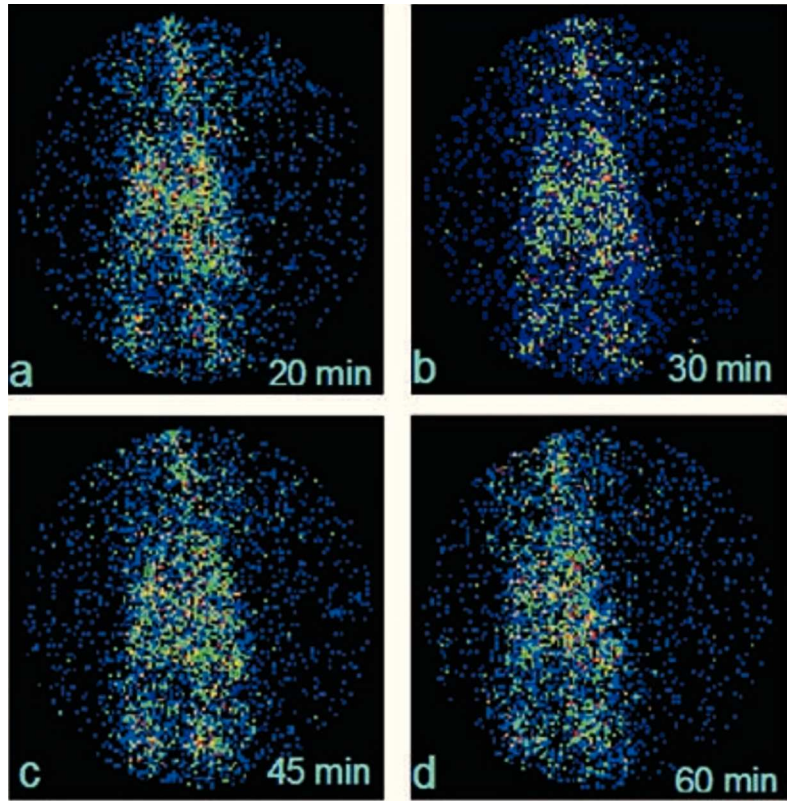

Fig. 17 – Images in posterior view, obtained after aerosol inhalation of ^{99m}Tc-HMPAO. The images didn't show any nodular localization, in spite of dispersed abdominal activity

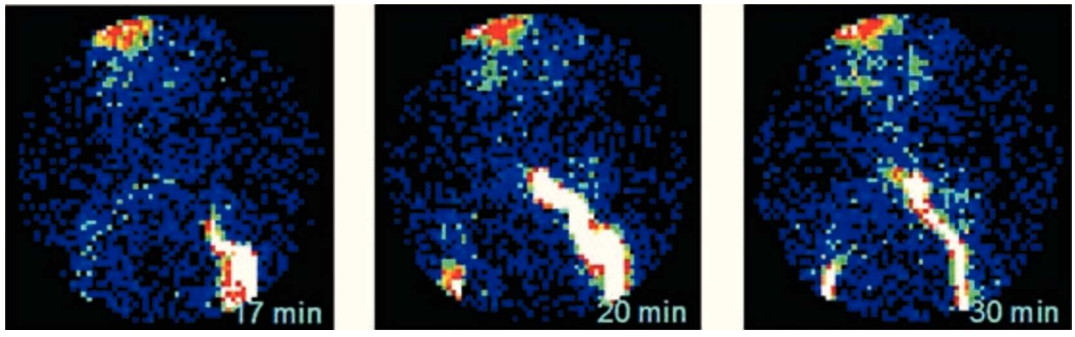

Fig. 18 – Images in anterior view of the pig n^{er} 15, obtained after interdigital injection in both the posterior members of nanocolloids of human albumin labelled with ^{99m}Tc

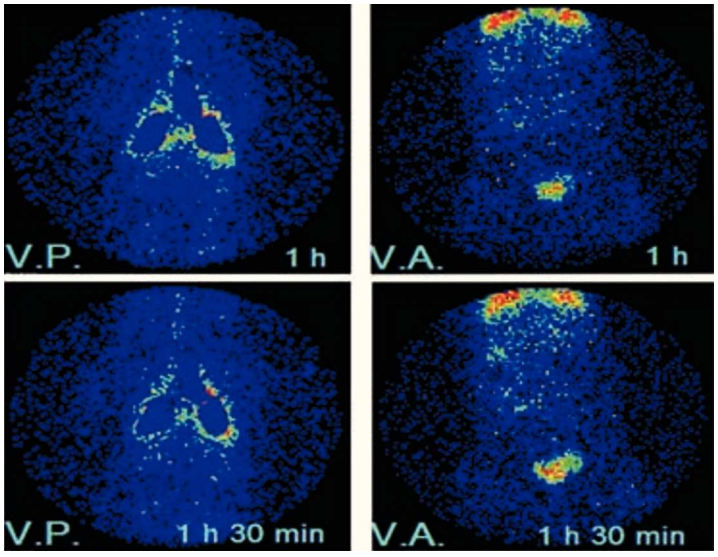

Fig. 19 – Images obtained 1 hour and 1.5 hours after 99mTc-liposome aerosol inhalation, in the animal nºr 23. The infradiaphragmatic, right renal hilum, pelvic region and bladder area localizations are apparent

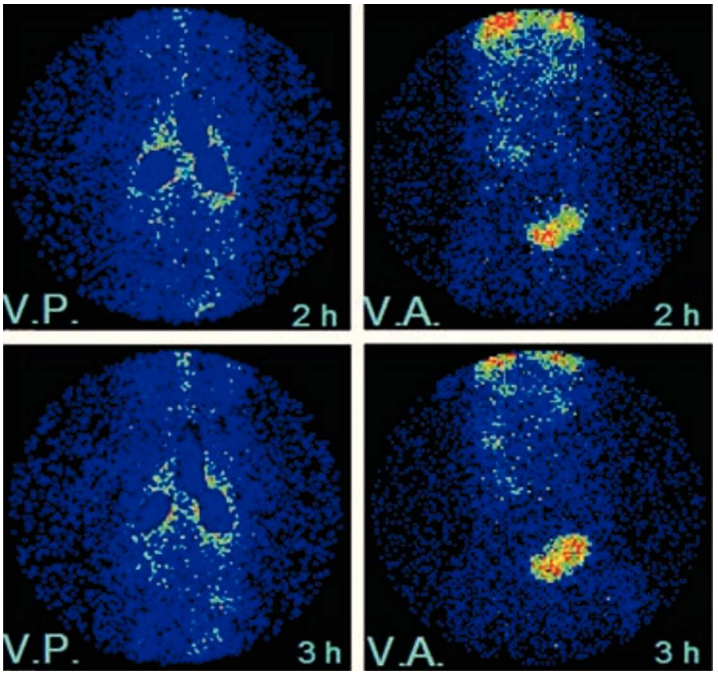

Fig. 20 – Images obtained at 2 and 3 hours after the ^{99m}Tc-liposome aerosol inhalation, in the animal nºr 23. The infradiaphragmatic, right renal hilum, pelvic region and bladder area localizations are much clearer

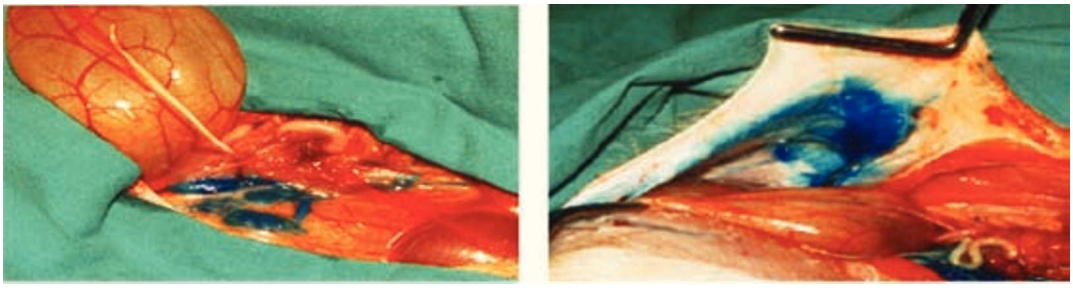

Fig. 21 – Early images of the indirect lymphography obtained after interdigital injection of methylene blue in the left inferior member

In the later times, the same two areas referred above were also directly visualised, but more intensively coloured by methylene blue (Fig. 22).

The comparison of the abdominal images obtained 60 minutes after liposomes labelled with ^{99m}Tc inhalation and 60 minutes after the indirect lymphoscintigraphy by interdigital injection of human albumin nanocolloids also labelled with ^{99m}Tc, allows to confirm that the visualized areas seemed to be in the same projections (Fig. 23).

Also in the animal n^{er} 23 crossed control studies of the *in vivo* liposomes stability were done. For this, during image acquisition blood samples were collected at 5 minutes, 30 min, 1, 2 and 3 hours after ^{99m}Tc-Liposomes inhalation. Urine was also obtained 3 hours after labelled liposomes inhalation. These samples were weighed, counted in a well counter and the specific counts calculated, which were converted into % of the injected activity (241 MBq), considering the 100% as the maximum lung activity.

As we can see in the graph of Fig. 24, the blood and urinary activity were particularly reduced, which indicates a good *in vivo* liposomes stability of formulation F.

In the animal n^{er} 23, we controlled through the images, the existence of lymphatic nodes areas corresponding to the presence of liposome in the systemic circulation, through venous return, as well as the activity corresponding to liposomal content leak, as result of biodegradation.

On the graph of Fig. 25 we can see the time distribution of the percentage of the admi-

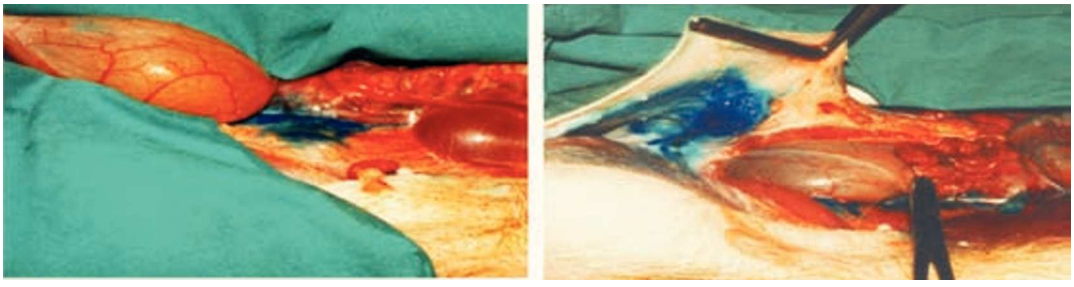

Fig. 22 – Delayed images of the indirect lymphography obtained after interdigital injection of methylene blue in the left inferior member

Maria Filomena Rabaça Roque Botelho, Maria Alcide Tavares Marques, Célia Maria Freitas Gomes, Augusto Marques Ferreira da Silva, Vasco António Andrade Figueiredo Bairos, Manuel Amaro de Matos Santos Rosa, Antero Pena Abrunhosa, João José Pedroso de Lima

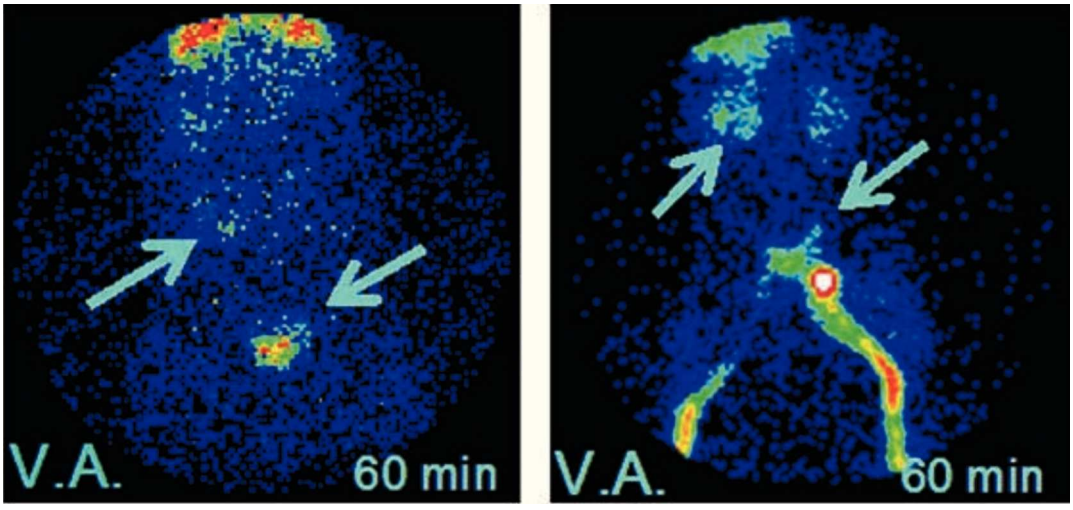

Fig. 23 – Abdominal scintigraphic images, obtained 60 minutes after liposome labelled with 99mTc inhalation (on the left) and 60 minutes after the interdigital injection of nanocolloids of human albumin labelled with 99mTc (on the right)

nistered activity in each ROI drawn in the images of the corresponding times to the blood and urine collections. As the normalization was made relatively to the pulmonary activity, considering the 100% as the maximum lung activity, we removed the lung column on the graph, allowing this way a better appreciation.

In Fig. 26, we can see another example, corresponding to the animal ner 18. After ^{99m}Tc-Liposome aerosols inhalation of formulation F the acquired images, without image processing, showed already visible lymphatic node areas. However, after image processing, this evidence was substantially improved.

In the image obtained 5 minutes (Fig. 26-a) after the inhalation, the hilar drainage chains are visualized, which became more individualised at 10 minutes (Fig. 26-b). At 13 minutes (Fig. 26-c) there was already transdiaphragmatic drainage, being clearly visible node areas in more delayed images (Fig. 26-d). At 25-27 minutes, aortic chain ganglia began to be visualised.

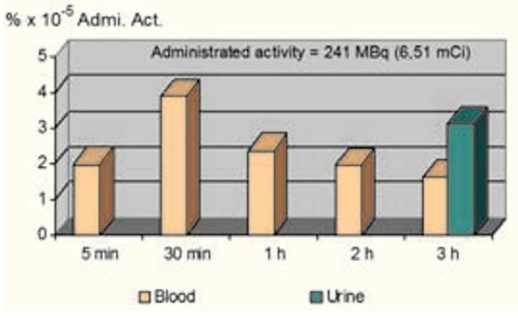

Fig. 24 – Graph that shows the % activity of the blood and urine samples, collected during images acquisition in the animal ner 23

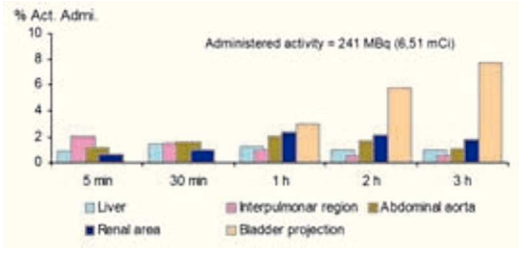

Fig. 25 – Graph that shows the time distribution of the % of administered activity, in each ROI in the animal nº 23. The column corresponding to the lung activity was excluded

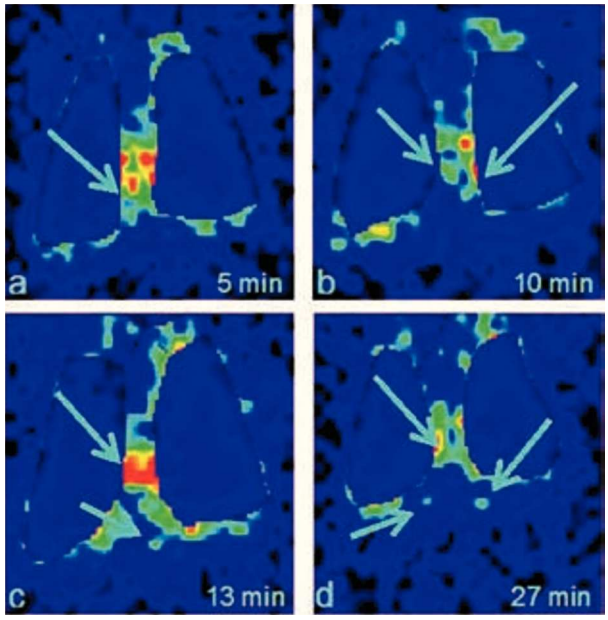

Fig. 26 – Thoracic images in posterior view obtained after ^{99m}Tc-Liposome aerosol inhalation, in the pig nº 18. a) 5 min after the inhalation – visualization of hilar draining chains; b) 10 min after the inhalation – individualisation of hilar draining chains; c) 13 min after the inhalation – transdiaphragmatic drainage; d) 30 min after the inhalation – initial visualization of the aortic chain ganglia

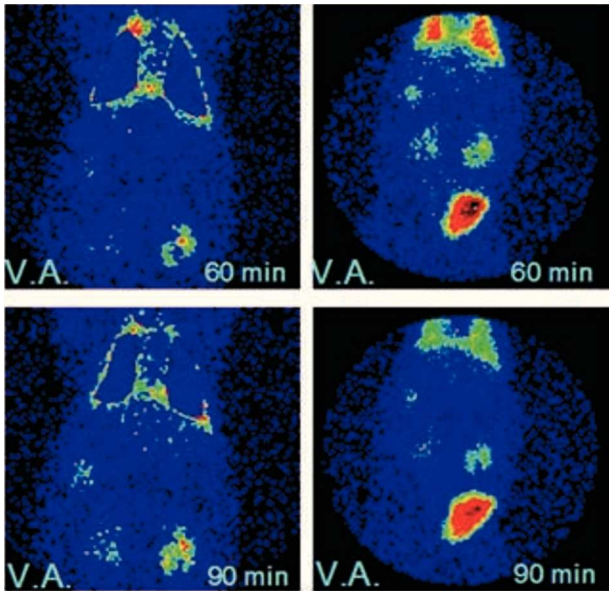

Fig. 27 – Images obtained 1 hour and 1.5 hours after the ^{99m}Tc-liposome aerosol inhalation, in the animal nºr 18. The infradiaphragmatic localizations, aortic chain, and in the renal projection areas, all over the ureter and in the bladder projection area are clear

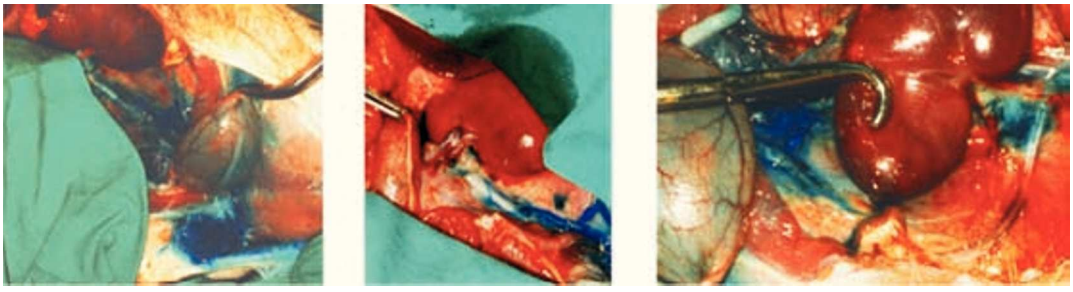

Fig. 28 – Images of the early times of the indirect lymphography obtained after interdigital injection of methylene blue in the left inferior member

In Fig. 27, we can observe the delayed images, both thoracic and abdominal, in anterior view, at 60 minutes and 90 minutes after liposomes inhalation. We can see the activity on the aortic chain, and on renal projection areas, including ureters and bladder projection.
These last localizations, that can put same interpretative doubts, are clarified by the direct visualization through indirect lymphography obtained after methylene blue interdigital injection (Fig. 28). In this image we can observe the lymphatic drainage vessels from the perivesical ganglia surrounding the ureter till the renal hilum.

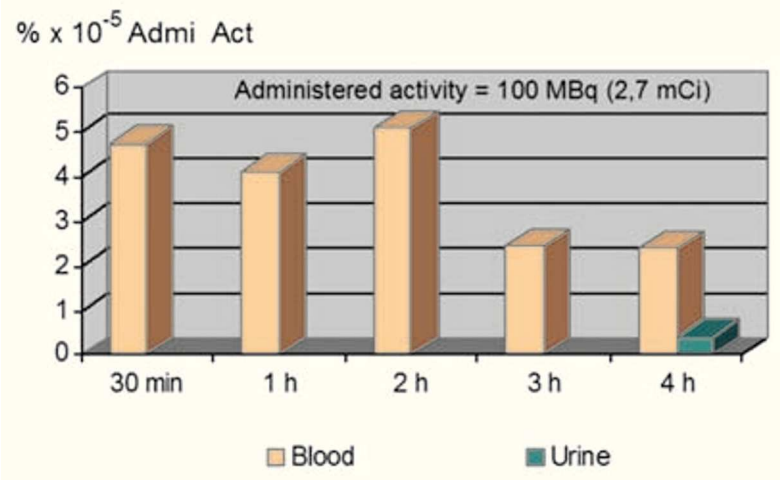

Fig. 29 – Graph that shows the percentual activity in the blood and urine samples, collected during the image acquisition in the animal nºr 18

Additionally, the blood and urine samples collected during the study, following the methodology described above, which results were presented as % of the maximum lung activity (100%) showed a very low blood pool activity, while in urine it was virtually insignificant (Fig. 29).
The percentual activity at the ROIs shows a similar distribution to the animal previously shown (Fig. 30).
The results obtained by analysis of blood and urine samples collected during the image acquisition, for a group of 8 pigs, can be observed in the graph of Fig. 31. These samples were weighed, counted in a well counter, normalized for the activity of a known sample and the average percentual activity was calculated considering as 100% the maximum lung activity.
As observed, there are some blood and urinary activity, but in very small amounts and clearly dependent on the water content leak by the liposomes, already analysed.

Discussion and conclusions

Liposomes production

The goal of this work was to produce and characterise liposomes that, after being

Maria Filomena Rabaça Roque Botelho, Maria Alcide Tavares Marques, Célia Maria Freitas Gomes, Augusto Marques Ferreira da Silva, Vasco António Andrade Figueiredo Bairos, Manuel Amaro de Matos Santos Rosa, Antero Pena Abrunhosa, João José Pedroso de Lima

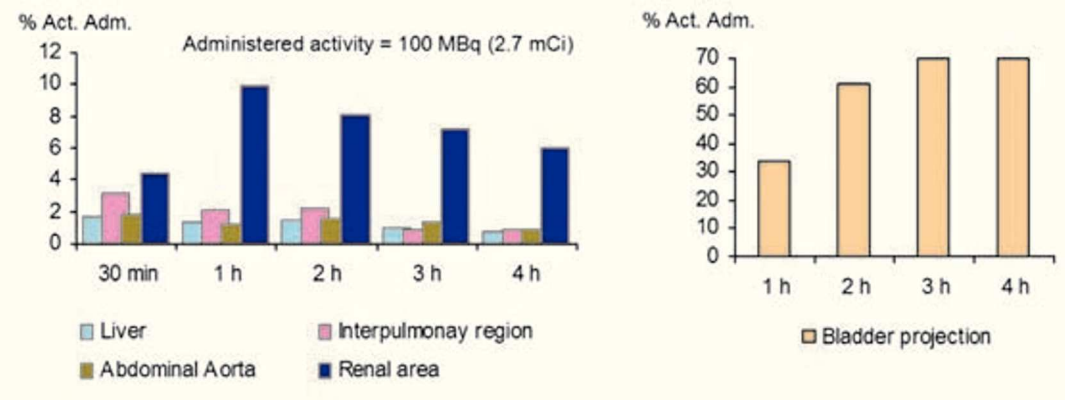

Fig. 30 – Time distribution of the percentual activity for liver, interpulmonary region, abdominal aorta and renal area (on the left) and for bladder projection (on the right) of the animal nᵉʳ 18

inhaled, would be preferentially cleared by the lung deep lymphatics.

The lymphatic system is of vital importance in the alveolar and interstitial clearance of a great diversity of substances (particles, dusts and pathogenic agents) that reach the alveoli, which must be removed in order to ensure gas exchange through the alveolar-capillary membrane.

The preferential lymphatic drainage of some microorganisms correlates with some specific surface components.

Several studies show a systematic and faster lymphatic removal of anionic than the cationic compounds with same molecular weight, which means that the pulmonary endothelium acts as a positive barrier[13]. This was the reason why the seven studied formulations present negative surface charge.

The liposomes preparation procedures must to obey to very restricted requirements. As our purpose was to obtain liposomes of similar dimensions of bacillus, but with a relatively high water core in order to retain the tracer, the unilamellar liposomes seemed to be the most appropriated. Additionally, as the used tracer to label the water phase was the ^{99m}Tc which has a physical radioactive period of 6 hours, the radionuclide encapsulation during the lipid film hydration was not convenient due to the long procedure time.

Keeping in mind these assumptions, the developed liposomes should be small, unilamellar, and would present some degree of negative surface charge in order to favour their lymphatic uptake[49]. On the other hand, the vesicles should be amenable to labelling, non-immunogenic and present enough stability to allow aerosolisation and the implementation of *in vivo* imaging studies[46].

As consequence, we choose the extrusion technique through polycarbonate membranes

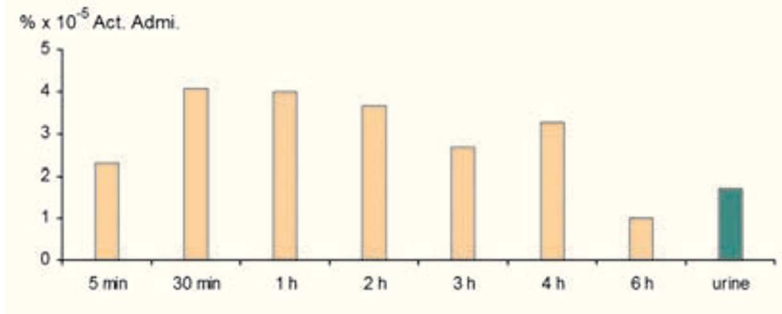

Fig. 31 – Graph showing the average percentual activity of the blood and urine samples, collected during the image acquisition for the group of 8 studied animals

with pores of 100 nm diameter and the labelling of the liposomes after its production, immediately before their administration.

According to several authors, repetitive extrusion of multilamellar vesicles above phase transition temperatures, provides an easy and reproducible method for producing unilamellar homogeneous vesicles of defined size from long-chain saturated phosphatidylcholines[8,26,27,28,41], without the need of organic solvents, detergents or sonication and with good encapsulation efficiencies. This choice was also reinforced by the fact that the small size liposomes radiolabelling efficiency was less then 5%, when the labelling procedure occurs during the hydration of the lipid films, before the vesicles formation[49].

Additionally, the fact of the extrusion under moderate pressures does not need organic solvent or detergents is another advantage, related to the small possibility of occurrence of inflammatory reactions of the bronchoalveolar epithelium, since these liposomes must be inhaled. The extrusion under moderate pressures can be applied to long chain saturated phospholipids as well, since the extrusion temperature will be higher then the phase transition temperature[17].

As we intended to use a fast and efficient labelling technique, our choice was ^{99m}Tc-HMPAO which is added to the reduced glutathione containing liposomes in the aqueous phase[25,38,50].

Although, in general terms, our results are in agreement with those obtained by other authors, some dependence of the labelling efficiency with the bilayer lipidic composition was observed (from 28.1 ± 4.3% for formulation E to 80.3 ± 15.3% for formulation F, as shown in Fig. 6), besides all formulations contained DSPC, a long chain saturated lipid. Related to the long chain saturated lipids, several authors recommended their use when stable liposomes are required, like when they are used as drug delivers. These lipids are also associated to bigger *in vivo* liposomes stability[17]. However, the addition of membrane stabilizers, like cholesterol and aminosugar derivatives[22,51,52] are other factors capable to influence the liposomes behaviour, as is confirmed by our results (Tables I and II).

The formulations with cardiolipin showed the smallest labelling efficiency, probably due to an excess of negative surface charge. Additionally, the presence of cholesterol alone does not appear to improve labelling efficiency (Formulation E = 28.1 ± 4.3%), unless a residue is added (Formulation G = 63.1 ± 21.8%). When the negative surface charge is decreased, using only PG as negative lipid (Formulations A, B and F), an increase in labelling efficiency is observed. However, there aren't significant differences in labelling efficiency among these formulations, which means that the choice of the residue is not a determinant factor.

It is also known that the *in vivo* liposomes stability is influenced not only by the lipidic composition but also, that can be modified by complement action, phospholipids interchanges and hydrophobic action of plasmatic proteins and phospholipases[14].

Our results of *in vivo* stability evaluation showed that the phospholipid composition and chemical properties of liposomal formulations determine its vulnerability to the disruptive effect of the human blood serum and plasma[14]. In fact, we verified that both human serum and plasma led to a decrease in the labelling efficiency of formulations C, D and E, although only formulation C presented statistically significant differences (t=2.4;

p=0.05 for human serum; t=2.0; p=0.05 for human albumin solution). All other formulations (A, B, F and G) showed an increase in labelling efficiency in the presence of human serum and plasma with statistically significant differences for formulations A (t=3.2; p=0.01 for human serum and plasma) and G (t=2.8; p=0.01 for human albumin solution). These results allow us to conclude that for these four formulations, the biological fluids do not induce leaks of its aqueous content.

The results of the stability studies associated to those of the labelling efficiency, allowed to exclude formulations C, D and E, once the chosen formulation must be stable and to have a good labelling efficiency. Moreover, formulation G was also discarded due to the presence of a potentially immunoreactive component (cardiolipin).

In order to assess the stability of the remaining formulations (A, B and F) to ultrasonic nebulisation, the labelling efficiency of these formulations was evaluated immediately after being submitted to 2.7 MHz ultrasound action for 2 minutes. The results obtained (Table II) didn't show any statistically significant differences in labelling efficiencies before and after ultrasound action[46,52,53]. This stability to ultrasound action is crucial, once its administration will be performed as an aerosol.

The three formulations were also assessed for loss of entrapped contents over 5.5 hours. This evaluation showed that formulation F presented the best performance, presenting the greater temporal stability, with almost no loss of aqueous contents (Fig. 7), which can be related with the simultaneous presence of cholesterol and N-acetyl muramic acid.

In opposition, less favourable stability results have been shown by formulation B, which differs from formulation F only by the absence of cholesterol whilst formulation A only had glutamic acid. According to this results, formulation F was selected as the most promising candidate.

The choice of correct lipid composition to produce liposomes as promising radiopharmaceutical carriers for visualization of lung lymphatics, to be administered as aerosols, must obey to several criteria: to be specifically drained by lung lymphatic vessels, to be easily and efficiently labelled, to be stable in presence of biological fluids, not induce immune response and to be resistant to ultrasound action. The results of *in vivo* tests described in chapter 3 allowed to conclude that formulation F (DSPC:PG:NAMA:CL) was the one that congregate the best characteristics for the considered goal. This formulation was submitted to other *in vitro* tests for a better physicochemistry characterization.

During the second passage of liposomes labelled with ^{99m}Tc-HMPAO by the Sephadex G25 column, for removing non encapsulated ^{99m}Tc-HMPAO, 120 fraction of 250µl were collected and counted in a well counter. The peak observed in Fig. 8 corresponds to the liposomes fraction that was eluted in the first 10 collected fractions. The activity counted in the remaining fractions corresponded to the not encapsulated tracer. This procedure assures that the collected labelled liposomes do not contain radiocontaminants, which is of high importance for the image quality of the lymphatic lung drainage, without artefacts, after administration as aerosol.

According to Nayar[17], the extrusion under moderate pressures and above lipids phase transition temperature, allows to get unila-

mellar liposomes of specific size, from saturated long chain phosphatidylcholines, without the use of organic solvents, detergents or sonication[29].

A molecular model of a small section of the formulation F vesicles outer layer can be seen in Fig. 4 in comparison with a model of a similar section of the *Bacillus subtilis* spore wall. Structures were energy minimized using a molecular mechanics (extended MM2) algorithm [CACHe, Oxford Molecular, Oxford, UK] until energy differences were below 0.01 kcal/mol.

The liposome mean diameter was measured in three fresh samples of the formulation F by quasi elastic light dispersion was 124 ± 32.1 nm with a polydispersity index of 0.09. Similar values were obtained after storage for 6 months at 4ºC (150.6 ± 48.2 nm with a polydispersity index of 0.17).

We prove that the maintenance of a homogeneous size during a period of 6 months can be related to the presence of the DSPC associated with small cholesterol percentage.

We also measured the electrophoretic mobility and zeta potential, both in fresh and after 6 months storage at 4ºC samples of liposomes of formulation F with Doppler laser. The results obtained confirmed the negative charge and showed no statistical significant differences before and after aging.

These results are of particular importance once they demonstrate the adequacy of the formulation for the production of a future kit for nuclear medicine studies for visualisation of the lung lymphatic drainage.

In summary, the developed liposomal formulation F demonstrated to have physicochemical and radiopharmaceutical properties that make it a very promising probe for molecular imaging studies of lung deep lymphatic chains. In addition, the labelled vesicles also displayed stability and toxicity profiles compatible with their human use for the evaluation of pulmonary lymphatic drainage in a standard diagnostic nuclear medicine environment.

In vivo studies

One of the goals of this work is to develop a methodology that allows, with a minimal invasion, to study the lung deep lymphatic drainage, which can be involved in several lung pathologies.

Also, the intention of administered the tracers as aerosols, is an important part of that goal. However, this implies that the liposomes that carry the gamma emitting molecules must reach juxta-alveolar lymphatics and the lymphatic capillaries associated to the respiratory bronchioles, i.e., the liposomes must reach the respiratory zone of the lung.

In general terms we can say that the particle deposition with diameters bigger than 1 µm occurs before the pulmonary compartment. Particles with diameters less than 1 µm are deposited in the pulmonary compartment, mainly by diffusion. Particles with a predominate dimension like the *bacilli* have a tendency to follow the aerodynamic flow, moving with its long axis parallel to the direction of the movement, which became more dependents on its small axis. This fact provokes a more peripheral deposition then expected[54].

As liposomes are sphere-shaped, oppositely to the *bacilli*, they must have diameters less then 1 µm, what it is in accordance with the dimensions obtained for liposomes of formulation F, when were measured by quasi

elastic light dispersion (average diameter = 124 ± 32.1 nm). With these dimensions, the liposomes have capacity to reach the pulmonary compartment, as it was confirmed by SEM analysis, carried out in rat lung, 20 minutes after inhalation of liposomes of formulation F.

Once reached the pulmonary compartment, the particle clearance to the juxta-alveolar lymphatics and the lymphatic capillaries associated with the respiratory bronchioles, can be carried by several forms[8]. With the developed liposomes, the SEM studies seem to prove that they can be phagocyted by alveolar macrophages (Fig. 15) or directly transferred through the intercellular junctions (Fig. 14) to the lung interstitium.

The indirect lymphoscintigraphic studies, carried out in 20 pigs, with liposomes of formulation F labelled with ^{99m}Tc-HM-PAO, showed that the alveolar clearance was relatively fast. In fact, the effective half-life at pulmonary level is of 45 minutes.

With this decay time, it is possible, as it proves the developed experimental model, the evaluation of the thoracic area. In the 20 pigs studied, the average times for lymphatic structures visualisation, after the liposomes inhalation, was of 5 minutes for the hilar and interpulmonary drainage chains. By this time, the transdiaphragmatic drainage chains are already delineated, being individualised approximately at 10 minutes. The ganglia of the aortic chain are visible at the 20 minutes and those of the renal hilar region by the 30 minutes.

We think that the visualization of descending transdiaphragmatic lymphatic drainage chains, easily after the aerosol inhalation, is important information given by this method. Simultaneously, the visualization of pelvic localizations at delayed times allowed us to suppose the presence of accessory lymphatic drainage chains that can be of great importance when a tumoral staging is needed.

The abdominal and pelvic localizations, namely the ones that correspond to the renal and bladder projection areas, put some interpretative problems. In fact, if the *in vitro* liposomes stability allows us to think in localization associated to the lymphatic drainage, the localizations themselves let us to think about *in vivo* liposomal degradation. To clarify this possibility, blood samples were collected at 5 min, 30 min, 1, 2 and 3 hours and urine samples at 3 hours after liposomes inhalation, in a group of 8 animals, during image acquisition period. The counts obtained through a well counter showed, after normalisation related to the administered activity, considering the 100% the maximum of the lung activity.

The irrelevant specific activity found in these samples (approximately 10^{-5} % of the administered activity) proves that the liposomes practically do not leak its aqueous content. This, being hydrosoluble, would pass to the blood, excreted through the kidney to the urine. Having practically no activity at blood and urine, the localizations at renal and bladder projections area, do not represent sanguineous or urinary activity.

This was confirmed by the indirect lymphographies with methylene blue, which by direct visualization of the lymphatic drainage clarified those localizations (Figs. 21, 22 and 28). Therefore, in the pelvic region we can see two blue coloured areas, one in the retrovesical region and another in the abdominal wall over the bladder and, in the renal projection area and renal hilum, an intense lymphatic network.

The analysis carried with the ROIs drawing in the acquired images, to verify if there was localizations corresponding to the presence of liposome in the systemic circulation through venous return as well as corresponding activity to the loss of the liposomal aqueous content by degradation, also confirmed our results.

Additionally, the localization of the abdominal lymphatic ganglia was confirmed by indirect lymphoscintigraphy with nanocolloids of human albumin labelled with technetium-99m, a specific tracer to lymphatic drainage and lymphatic ganglia. The comparison of these images, with those obtained with liposome aerosols allowed us to say that after 1.5 hours, no significant information is added. On account of this, the time required to the scintigraphy is relatively short.

To ensure the fiability of the results, data was statistically analysed, based on the activities detected in the nodes localizations as well as on the background activity. The signal-noise relationship of the lymphatic nodes, at the maximum activity timing, showed values that fluctuate from 5 times to some orders of magnitude, being the statistical errors systematically inside of the acceptable limits in experimentation.

As conclusion we can affirm that the developed liposomal formulation F demonstrated to have physicochemical and radiopharmaceutical properties that make it a very promising probe for molecular imaging studies of lung deep lymphatic chains. In addition, the labelled vesicles also displayed stability and toxicity profiles compatible with their human use for the evaluation of pulmonary lymphatic drainage in a standard diagnostic nuclear medicine environment.

In general terms, we can say that when pulmonary pathology is associated with deep lymphatic involvement, its study is possible and useful, and the presented method is a real possibility. It seems that the visualisation of the early descending transdiaphragmatic drainage chains, adds important information that can be crucial when an accurate tumoral staging is need.

Keeping in mind the stability characteristics along the time, these liposomes can be made and stored, as a kit, ready to use.

The developed methodology of labelling after liposomes production, like a cold radiopharmaceutical kit ready to radiolabelling, facilitates a lot its practical application.

This technology of nanoradioliposomes molecularly modulated, with specificity for organs or tissues can open new perspectives in diagnostic and therapeutic techniques.

In fact, this work showed that is possible to produce nanoradioliposomes targeting organs or tissues, not only for basic investigation but also with diagnostic and/or therapeutic purposes. This assumption is confirmed by the versatility induced by this modulation technique. In the future, their use could maximise the drug actions or even potentiate them, minimising the collateral effects.

Aknowledgments

We want to thank to a group of persons who direct and indirectly helped to accomplish the presented work.

Prof. Doutor João Patrício, Director of the Experimental Investigation Laboratory, from Coimbra University Hospitals, as well as Ms. Maria de Lurdes Silva and Mr. Carlos Silva.

Prof. Doutor Carlos Gonçalves from Histology and Embriology Institute of Faculty of Medicine of Coimbra University.

Drª. Vera Fonseca from Immunology Institute of Faculty of Medicine of Coimbra University.
Drª. Cristina Fonseca from Faculty of Pharmacy of Coimbra University.
Prof. Doutora Margarida Figueiredo and Eng. Maria José Moura from Pedro Nunes Institute, Coimbra.

Bibliography

1. DG Bishop, L Rutberg, B Samuelsson. The chemical composition of the cytoplasmic membrane of *Bacillus subtilis.* Eur J Biohem 1967;2:448-453.
2. JAF Op der Kamp, I Redai, LLM van Deenen, Phosholipid composition of *Bacillus subtilis*. J Bacteriol 1969;99:298-303.
3. DC McPherson, H Kim, M Hahn, R Wang, P Grabowski, P Eichenberger, A Driks1. Characterization of the *Bacillus subtilis* spore morphogenetic coat Protein CotO J Bacteriol 2005;187:8278–8290.
4. V Leak, VJ Ferrans. Lymphatics and lymphoid tissue, *in:* RG Crystal, JB West, *et al.* (Eds.), The Lung: Scientific Foundations, Raven Press Ltd, New York, 1997, pp.779-786.
5. AE Taylor, JW Barnard, SA Barman, WK Adkins, Fluid Balance, *in:* RG Crystal, JB West, *et al.* (Eds.). The Lung: Scientific Foundations, Raven Press Ltd, New York, 1997:1147-1161.
6. C Nagaishi, Y Okada. The pulmonary lymphatic system, *in:* AP Fishman's Pulmonary Disease and Disorders, Vol.2, JD Dereck, M Navrozov (Eds.) London, McGraw-Hill Inc, 1980:901-908.
7. AP Fishman. Pulmonary edema, *in:* AP Fishman's Pulmonary Disease and Disorders, Vol.2, J.D. Dereck, M Navrozov (Eds.) London, McGraw-Hill Inc, 1980: 919-952.
8. JM Lauweryns, JH Baert. Alveolar clearance and the role of the pulmonary lymphatics. Am Rev Respir Dis 1977;115:625-683.
9. T Grant, B Levin. Lymphangiographic visualization of pleural and pulmonary lymphatics in a patient without chylothorax. Radiology 1974;113:49-50.
10. J Liua, Ho-Lun Wong, Moselhyc, B Bowenc, XY Wuc, MR Johnston. Targeting colloidal particulates to thoracic lymph nodes. Lung Cancer 2006;51: 377-386.
11. RS Hanson, JA Peterson, AA Yousten. Unique biochemical events in bacterial sporulation, Annu Rev Microbiol 1970;24:53-90.
12. AI Aronson, P Fitz-James. Structure and morphogenesis of the bacterial spore coat. Bacteriol Rev 1976;40:360-402.
13. JC Parker. Transport and distribution of charged macromolecules in lung. Adv Microcirc 1987;13:150-159.
14. MC Finkelstein, G Weissmann. Enzyme replacement via liposomes. Variations in lipid composition determine liposomal integrity in biological fluids. Biochim Biophys Acta 1979;587:202-216.
15. Gregoriadis, J Senior. The phospholipid component of small unilamellar liposomes controls the rate of clearance of entrapped solutes from the circulation. FEBS Letters 1980;119:43-46.
16. MR Zalustry, MA Noska, PW Gallagher. Properties of multilamellar liposomes containing 99mTcO4-: Effect of distearoylphosphatidylcholine to sphingomyelin ratio. J Nucl Med 1986;13:269-276.
17. R Nayar, MJ Hope, PR Cullis. Generation of large unilamellar vesicles from long-chain saturated phosphatidylcholines by extrusion techniques. Biochim Biophys Acta 1989;986:200-206.
18. C Oussoren, G Storm. Targeting to lymph nodes by subcutaneous administration of liposomes. Inter J Pharma 1998;162:39-44.
19. WT Phillips, R Klipper, B Goins. Novel method of greatly enhanced delivery of liposomes to lymph nodes1. JPET 2000;295:309-313.
20. W Yan, L Huang. Recent advances in liposome-based nanoparticles for antigen delivery. Polymer Reviews 2007;47:329-344.
21. DA Tyrrell, TD Heath, CM Colley, BE Ryman. New aspects of liposomes. Biochim Biophys Acta 1976;457:259-302.
22. C Kirby, J Clarke, G Gregoriadis. Effect of the cholesterol content of small unilamellar liposomes on their stability in vivo and in vitro. Biochem J 1980;186:591-598.
23. MR Mauk, RC Gamble. Preparation of lipid vesicles containing high levels of entrapped radioactive cations. Anal Biochem 1979;94:302-307.
24. P Osborne, VJ Richardson, K Jeysingh, BE Ryman. Radionuclide-labelled liposomes – A new lymph node imaging agent. Int J Nucl Med 1979;6:75-83.
25. WT Phillips, AS Rudolph, B Goins, JH Timmons, R Klipper, R Blumhardt. A simple method for produc-

ing technetium-99m-labeled liposome which is stable in vivo. Nucl Med Biol 1992;19:539-547.
26. MR Jacquier-Sarlier, BS Polla, DO Slosman. Oxidoreductive state: the major determinant for cellular retention of technetium-99m-HMPAO. J Nucl Med 1996;37:1413-1416.
27. B Goins, WT Phillips, R Klipper. Blood-pool imaging using technetium-99m-labeled liposomes. J Nucl Med 1996;37:1374-1379.
28. VD Awashi, B Goins, R Klipper, WT Phillips. Dual radiolabeled liposomes: biodistribution studies and localization of focal sites of infection in rats. Nucl Med Biol 1998;25:155-160.
29. RC MacDonald, RI MacDonald, BPM Menco, K Takeshita, NK Subbarao, L-R Hu. Small-volume extrusion apparatus for preparation of large unilamellar vesicles. Biochim Biophys Acta 1991;1061:297--303.
30. F Olson, CA Hunt, FC Szoka, WJ Vail, D Papahadjopoulos. Preparation of liposomes of defined size and distribution by extrusion through polycarbonate membranes. Biochim Biophys Acta 1979;557:9-23.
31. MJ Hope, MB Bally, G Webb, PR Cullis. Production of large unilamellar vesicles by a rapid extrusion procedure: characterization of size distribution, trapped volume and ability to maintain a membrane potential. Biochim Biophys Acta 1985;812:55-65.
32. C Huang. Studies on phosphatidylcholine vesicles. Formation and physical characteristics. Biochemistry 1969;8:344-351.
33. IR McDougall, JK Dunnick, ML Goris, JP Kriss. In vivo distribution of vesicles loads with radiopharmaceuticals: a study of different routes of administration. J Nucl Med 1975;16:488-491.
34. LA Medina, R Klipper, WT Phillips, B Goins. Pharmacokinetics and biodistribution of [111In]-avidin and [99mTc]-biotin-liposomes injected in the pleural space for the targeting of mediastinal nodes. Nucl Med Biol 2004;31:41-51.
35. WT Phillips, R Klipper, B Goins. Use of 99mTc-labeled liposomes encapsulating blue dye for identification of the sentinel lymph node. J Nucl Med 2001; 42:446-451.
36. F Ahkong, C Tilcock. Attachment of 99mTc to lipid vesicles containing the lipophilic chelate dipalmitoylphosphatidylethanolamine-DTTA. Nucl Med Biol 1992; 19:831-840.
37. LP Kasi, G Lopez-Berestein, K Mehta, M Rosenblum, HJ Glenn, TP Haynie, G Mavligit, EM Hersh. Distribution and pharmacology of intravenous 99mtc-labeled multilamellar liposomes in rats and mice. Int J Nucl Med Biol 1984;11: 35-37.
38. B Goins, R Klipper, AS Rudolph, WT Phillips. Use of technetium-99m-liposomes in tumor imaging J Nucl Med 1994;35:1491-1498.
39. SM Saari, MT Vidgren, MO Koskinen, VMH Turjanmaa, JC Waldrep, MN Nieminem. Regional lung deposition and clearance of 99mTc-labeled beclomethasone-DLPC liposomes in mild and severe asthma. Chest 1998;113:1573-1579.
40. P Shurtenberger, H Hauser. Characterization of the size distribution of unilamellar vesicles by gel filtration, quasi-elastic light scattering and electron microscopy. Biochim Biophys Acta 1984;778:470-480.
41. G Perevucnik, P Schurtenberger, H Hauser. Size analysis of biological membrane vesicles by gel filtration, dynamic light scattering and electron microscopy. Biochim Biophys Acta 1985;821:169-173.
42. LD Mayer, MJ Hope, PR Cullis. Vesicles of variable sizes produced by a rapid extrusion procedure. Biochim Biophys Acta 1986;858:161-168.
43. DJ Hnatowich, B Clancy. Investigations of a new, highly negative liposome with improved biodistribution for imaging. J Nucl Med 1980;21:662-669.
44. KMG Taylor, G Taylor, IW Kellaway, J Stevens. The stability of liposomes to nebulization. Int J Pharm 1990;58:57-61.
45. RW Niven, H Schreier. Nebulization of liposome. I. Effects of lipid composition. Pharm Res 1990;7:1127-1133.
46. KKM Leung, PA Bridges, KMG Taylor. The stability of liposomes to ultrasonic nebulization. Int J Pharm 1996;145:95-102.
47. S Thomas, H Atkins, J McAfee, MD Blaufox, M Fernandez, PT Kirchner, RC Reba. Radiation absorbed dose from tc-99m diethylenetriaminepentaacetic acid (DTPA). J Nucl Med 1984;25:503-505.
48. International Commission of Radiation Protection Publication 30. New York, Pergamon Press, 1988.
49. VJ Caride. Technical and biological considerations on the use of radiolabeled liposomes for diagnostic imaging. Nucl Med Biol 1990;17:35-39.
50. B Goins, R Klipper, AS Rudolph, RO Cliff, R Blumhardt, WT Phillips. Biodistribution and ima-

ging studies of technetium-99m-labeled liposomes in rats with focal infection. J Nucl Med 1993;34:2160--2168.
51. JH Crowe, LM Crowe, JF Carpenter, AS Rudolph, CA Wistrom, BJ Spargo, TJ Anchordoguy. Interactions of sugars with membranes. Biochim Biophys Acta 1988;947:367-384.
52. RP Goodrich, TM Handel, JD Baldeschwieler. Modification of lipid phase behavior with membrane-bound cryoprotectants. Biochim Biophys Acta 1988; 938:143-154.
53. ONM Mc Callion, KMG Taylor, M Thomas, AJ Taylor. Nebulization of monodisperse latex sphere suspensions in air-jet and ultrasonic nebulizers. Int J Pharm 1996;133:203-214.
54. RF Phalen. Basic morphology and physiology of the respiratory tract, *in:* Inhalation Studies: Foundations and techniques. CRC Press, Boca Raton, Florida, 1984:51.